

Copyright

By

Taner Sensoy

2009

Use of Nanoparticles for Maintaining Shale Stability

By

Taner Sensoy, B.Sc.

Thesis

Presented to the Faculty of the Graduate School

of The University of Texas at Austin

in Partial Fulfillment

of the Requirements

for the Degree of

Master of Science in Engineering

The University of Texas at Austin

May 2009

Use of Nanoparticles for Maintaining Shale Stability

APPROVED BY

SUPERVISING COMMITTEE

Martin E. Chenevert, Supervisor

Mukul M. Sharma, Co-Supervisor

Dedication

I would like to dedicate this thesis to Mustafa Kemal Atatürk, the eternal leader of Turkish Nation, revolutionary statesman, and founder of the Republic of Turkey.

Acknowledgements

I would like to thank Dr. Martin E. Chenevert and Dr Mukul M. Sharma for their excellent guidance, with their technical and personal experiences throughout this research.

Moreover, I would like to thank Dr. Tadeusz W Patzek, for his kind help and interest in my research.

Finally, I would also like to thank Glen Baum, Gary J. Miscoe and Collins Osuji for all their excellent support during this study.

Use of Nanoparticles for Maintaining Shale Stability

By

Taner Sensoy, M.S.E.

The University of Texas at Austin, 2009

SUPERVISOR: Martin E. Chenevert and Mukul M. Sharma

This experimental study presents the effect of adding nanoparticles to water-based drilling muds and their effect on fluid penetration into hard and soft shale. Use of water-based muds during drilling can cause fluid penetration from the mud into shale formations resulting in swelling and wellbore instability. The nanometer sized pore throat diameters in shales are too small for conventional drilling fluid particles to invade and build a mud cake. Nanoparticles in the shale pore size range were added to lab and field muds to effectively reduce fluid invasion. The sensitivity of nanoparticle dispersions to temperature and salt concentration in the mud was also determined. Four different field muds were studied with and without the addition of nanoparticles using Atoka and Gulf of Mexico shales. Penetration of fluids into the shales was shown to decrease dramatically when nanoparticles were properly sized and applied.

Results show that nanoparticles reduce the permeability of the Atoka shale by a factor of 5 to 50. Similar results are obtained for the GOM shale. Using a nanoparticle

dispersion, water penetration into Atoka shale was reduced by 98% as compared to sea water. The membrane efficiency of the shale (a measure of the osmotic pressure contribution) was found to increase by an order of magnitude. Scanning electron micrographs of the Atoka shale taken after exposure to nanoparticle dispersions show that the nanoparticles do indeed penetrate and plug the shale pore throats. These results suggest that nanoparticles could significantly reduce wellbore instability problems in reactive shales.

This plugging of pore throats by the use of nanoparticles is a new approach for controlling fluid invasion into shales, and could have a major impact on solving the chronic problem of wellbore instability.

Table of Contents

List of Tables	x
List of Figures	xii
Chapter 1 Introduction	1
Chapter 2 Shale Properties.....	3
2.1 Atoka shale.....	3
2.2 C5 shale.....	5
2.3 Gulf of Mexico shale (GOM)	6
Chapter 3: Field Muds and Nanoparticle Properties.....	8
3.1 Field Mud Properties.....	8
3.2 Nanoparticle Properties.....	9
Chapter 4: Problem Statement, Test Procedure and Data Evaluation	11
4.1 Problem Statement.....	11
4.2 Test Procedure	12
4.3 Data Evaluation.....	13
Chapter 5: Preliminary Testing.....	19
5.1 Swelling Test	19
5.2 Multi-step Tests	20
5.3 Nanoparticle Concentration Tests.....	25
5.4 Scanning Electron Micrographs.....	30
5.5 Nanoparticle Type and Size Tests.....	32
Chapter 6: Field Mud Tests.....	35
6.1 Field Muds in contact with Atoka shale	35
6.2 Field Muds in contact with GOM shale.....	50
Chapter 7: Conclusions and Future Work.....	67

Appendix A	69
Bibliography	79
Vita	80

List of Tables

Table 2.1:	Composition of Atoka shale.....	4
Table 2.2:	Composition of C5 shale.....	5
Table 2.3:	Native water activity data of GOM shale	6
Table 3.1:	Field Muds properties	8
Table 3.2:	Properties of the field muds modified with NP	9
Table 3.3:	Precipitation temperatures of NP dispersions.	10
Table 5.1:	3M two steps test in contact with Atoka shale.....	21
Table 5.2:	3M 20 nm two step test in contact with Atoka shale	23
Table 5.3:	3M 20 nm three steps test on C5 shale	24
Table 5.4:	3M 20 nm 29 wt % test in contact with Atoka shale	26
Table 5.5:	3M 20 nm 5 wt % test in contact with Atoka shale	27
Table 5.6:	3M 20 nm 10 wt % test in contact with Atoka shale	28
Table 5.7:	Conditions for Test 5.7	33
Table 5.8:	Conditions for Test 5.8 and 5.9.....	34
Table 6.1:	Conditions for Test 6.1	36
Table 6.2:	Conditions for Test 6.2	38
Table 6.3:	Mud composition in Test 6.2	38
Table 6.4:	Conditions for Test 6.3	39
Table 6.5:	Conditions for Test 6.4	41
Table 6.6:	Mud composition in Test 6.4	42
Table 6.7:	Conditions for Test 6.5	43
Table 6.8:	Conditions for Test 6.6	45

Table 6.9: Mud composition in Test 6.6	45
Table 6.10: Conditions for Test 6.7	46
Table 6.11: Conditions for Test 6.8	48
Table 6.12: Mud composition in Test 6.8	49
Table 6.13: Permeability values obtained with and without NP for Atoka	49
Table 6.14: Conditions for Test 6.9	51
Table 6.15: Conditions for Test 6.10	53
Table 6.16: Mud composition in Test 6.10	54
Table 6.17: Conditions for Test 6.11	55
Table 6.18: Conditions for Test 6.12	57
Table 6.19: Mud composition in Test 6.12	57
Table 6.20: Conditions for Test 6.13	58
Table 6.21: Conditions for Test 6.14	60
Table 6.22: Mud composition in Test 6.14	61
Table 6.23: Conditions for Test 6.15	62
Table 6.24: Conditions for Test 6.16	64
Table 6.25: Mud composition in Test 6.16	64
Table 6.26: Conditions for Test 6.17	65
Table 6.27: Permeability values obtained with and without NP for GOM	66

List of Figures

Figure 2.1: Native water activity of Atoka shale.....	4
Figure 2.2: Saturation test of Atoka shale	5
Figure 2.3: Native water activity of C5 shale.....	6
Figure 2.4: Native water activity of GOM shale	7
Figure 4.1: Particle Size Scale.....	11
Figure 4.2: Test cell used in the tests	13
Figure 4.3: Differential pressure example	14
Figure 4.4: Example 1 test result.....	16
Figure 4.5: Example 2 test result.....	16
Figure 4.6: Example 3 test result.....	17
Figure 5.1: C5 Shale swelling test performed with water and NP dispersion.....	20
Figure 5.2: Three steps test in contact with Atoka shale.....	21
Figure 5.3: Two step test with and without NP	22
Figure 5.4: Three-steps test with C5 shale without and with NP	24
Figure 5.5: Results of the test which was performed with 29 wt %	25
Figure 5.6: Results of the test which was performed with 5 wt %	27
Figure 5.7: Results of the test which was performed with 10 wt %	28
Figure 5.8: NP tests with different concentrations in contact with Atoka.....	29
Figure 5.9: SEM of 20 nm particles in contact with Atoka shale.....	30
Figure 5.10: 20 nm silica NP in different scale	31
Figure 5.11: Group of particles plugged a pore throat.	31
Figure 5.12: Results of the Test 5.7 , Nyacol 40 wt % 20 nm dispersion	32
Figure 5.13: 3M's 17 wt % and Nyacol's 15 wt % 5 nm dispersions on Atoka ...	34

Figure 6.1: Results of Test 6.1 that was performed in contact with Atoka	35
Figure 6.2: Results of Test 6.2 that was performed in contact with Atoka	37
Figure 6.3: Comparison of Mud A with and without NP in contact with Atoka	37
Figure 6.4: Results of Test 6.3 that was performed in contact with Atoka.....	39
Figure 6.5: Results of Test 6.4 that was performed in contact with Atoka.....	40
Figure 6.6: Comparison of Mud B with and without NP in contact with Atoka ..	41
Figure 6.7: Results of Test 6.5 that was performed in contact with Atoka.....	42
Figure 6.8: Results of Test 6.6 that was performed in contact with Atoka.....	43
Figure 6.9: Comparison of Mud C with and without NP in contact with Atoka ..	44
Figure 6.10: Results of Test 6.7 that was performed in contact with Atoka.....	46
Figure 6.11: Results of Test 6.8 that was performed in contact with Atoka.....	47
Figure 6.12: Comparison of Mud D with and without NP in contact with Atoka.	48
Figure 6.13: Permeability chart of Atoka	50
Figure 6.14: Results of Test 6.9 that was performed in contact with GOM.....	51
Figure 6.15: Results of Test 6.10 that was performed in contact with GOM.....	52
Figure 6.16: Comparison of Mud A with and without NP in contact with GOM	.53
Figure 6.17: Results of Test 6.11 that was performed in contact with GOM.....	54
Figure 6.18: Results of Test 6.12 that was performed in contact with GOM.....	56
Figure 6.19: Comparison of Mud B with and without NP in contact with GOM	.56
Figure 6.20: Results of Test 6.13 that was performed in contact with GOM...58	
Figure 6.21: Results of Test 6.14 that was performed in contact with GOM ...59	
Figure 6.22: Comparison of Mud C with and without NP in contact with GOM	.60
Figure 6.23: Results of Test 6.15 that was performed in contact with GOM....61	
Figure 6.24: Results of Test 6.16 that was performed in contact with GOM	63

Figure 6.25: Comparison of Mud D with and without NP in contact with GOM	63
Figure 6.26: Results of Test 6.17 that was performed in contact with GOM.....	65
Figure 6.27: Permeability chart of GOM.....	66
Figure A1: Circular 6" saw.....	69
Figure A2: Plastic tube placed on a base covering the shale column.	70
Figure A3: The plastic tube containing shale and sandstone, filled with epoxy.....	71
Figure A4: Circular 12" saw	72
Figure A5: Final appearance of the shale disc ready to be placed in desiccators	72
Figure A6: Desiccators	73
Figure A7: Configuration of the test device	74
Figure A8: Test cell	75
Figure A9: Manual pump.....	76
Figure A10: Syringe pump	77
Figure A11: Data accumulation system	78

Chapter 1

Introduction

Maintaining wellbore stability is one of the most critical aspects of drilling. Water invasion into the shale formation weakens the wellbore and causes problems such as hole collapse, and stuck pipe. The extremely low permeability and low pore throat size of shale is such that normal filtration additives do not form mud cakes and thus do not stop fluid invasion. This research aims to reduce shale permeability by using nanoparticles to plug pore throats, build an internal mud cake and thereby reduce the fluid invasion into the shale.

Recent work¹ has shown that reducing the permeability of shale can enhance its membrane efficiency; thus it is also possible that placing nanoparticles in salt water muds could increase the mud's membrane efficiency.

It is accepted that balanced activity oil-continuous mud is a good solution to the shale stability problem since there is no chemical interaction between oil and shale, and the water can be made immobile using emulsified saline water droplets.² However, a solution for water-based muds (WBM) is needed, especially in environmentally sensitive areas. Even though there have been many studies that focus on improving the hole stability properties of WBM, no such inhibited mud exists. It is thought that pore throat plugging has not been achieved in the past because the size of the solid mud additives currently used is too large to plug nanometer sized pore throat openings.

Properties of the shales, nanoparticles, and muds used in this study will be presented first. A statement of the problem, test procedures used in the experiments and data evaluation methods are presented next. The results of the preliminary tests are presented in Chapter 5.

The results of the field mud tests with and without nanoparticles are presented for Atoka and Gulf of Mexico shales in Chapter 6. Results are compared for each field mud to show the effect of nanoparticles for both Atoka and Gulf of Mexico shales. Finally conclusions are presented.

Chapter 2

Shale Properties

Shale is a sedimentary rock that is formed by clays, quartz, and other minerals that are found in fine-grained rocks. Because of its high clay content, shale tends to absorb water from a WBM, which results in swelling and wellbore failure. As Al-Bazali³ states, shales that contain smectite or montmorillonite clays can absorb huge amounts of water. Hence shale type and composition play a critical role in wellbore stability problems.

There are three types of shales being tested, Atoka, C5, and Gulf of Mexico (GOM). Mineralogical compositions and native activities of the shale types play key roles in the shale stability problem. Shales with a higher clay content, show a higher tendency to absorb water.

2.1 Atoka Shale

The mineralogical composition of Atoka shale is shown in Table 2.1. Atoka is considered to be a hard shale. In earlier work, Osuji¹ has shown in his Atoka shale study that at its native water activity of 0.72 it is saturated with water. As shown in Figure 2.1, by changing the activity of the sample, weight differences were recorded and plotted. As the point in Figure 2.1 (where the sample did not gain or lose moisture), the native water activity of the sample was determined. As shown in Figure 2.2, by changing the water content of the shale and then determining the resulting volume change by an oil-immersion method and a weight change method, it was determined that there was no air

in the shale, which means that the shale is fully saturated. Details of this method are provided in Reference 1.

Table 2.1: Composition of Atoka shale

X-Ray Diffraction	Wt %
Quartz	52
Feldspar	15
Total Clay	33
Kaolinite	32
Chlorite	7
Illite	31
Smectite	19
Mixed Layer	11

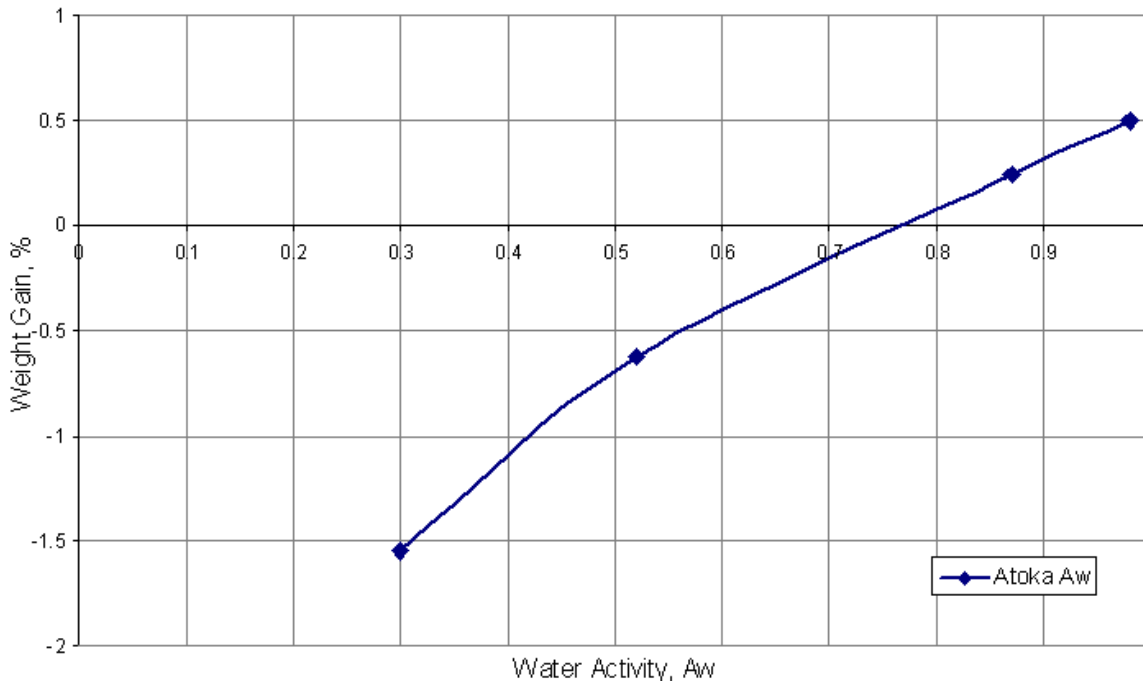


Figure 2.1: Native water activity of Atoka shale¹

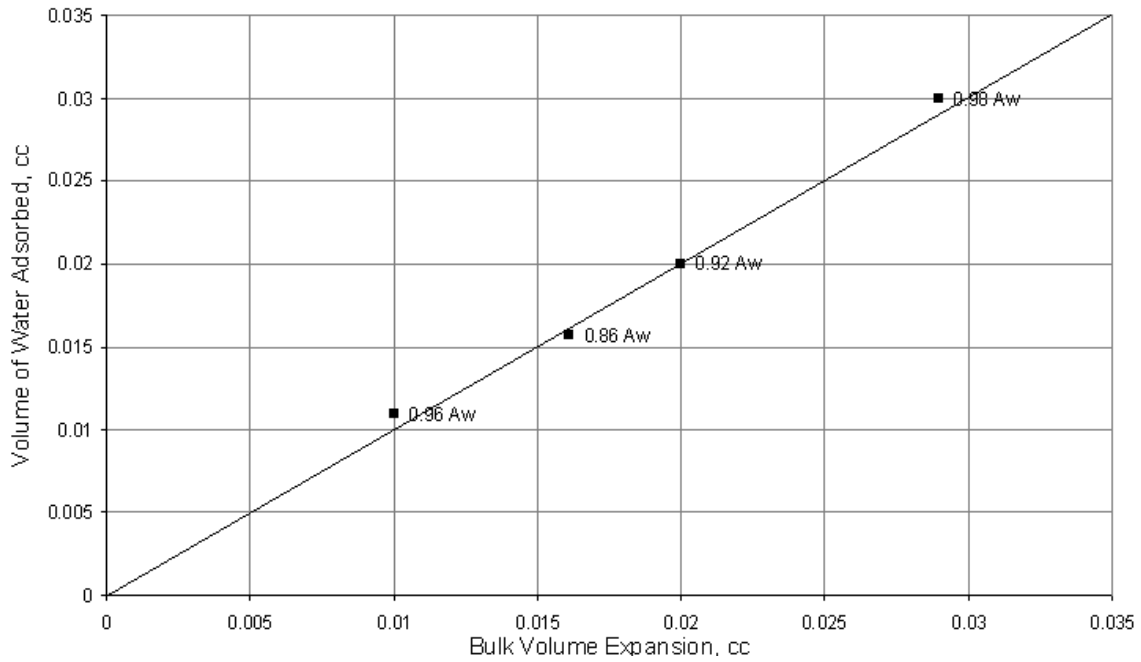


Figure 2.2: Saturation Test of Atoka shale

2.2 C5 Shale

The mineralogical composition and native activity of C5 shale obtained from Chevron is shown in Table 2.2 and Figure 2.3. The C5 shale, which has a higher clay content, is considered to be a soft shale.

Table 2.2: Composition of C5 shale

X-Ray Diffraction	Wt %
Quartz	32
Feldspar	24
Total Clay	44
Kaolinite	50
Chlorite	1
Illite	13
Smectite	7
Mixed Layer	29

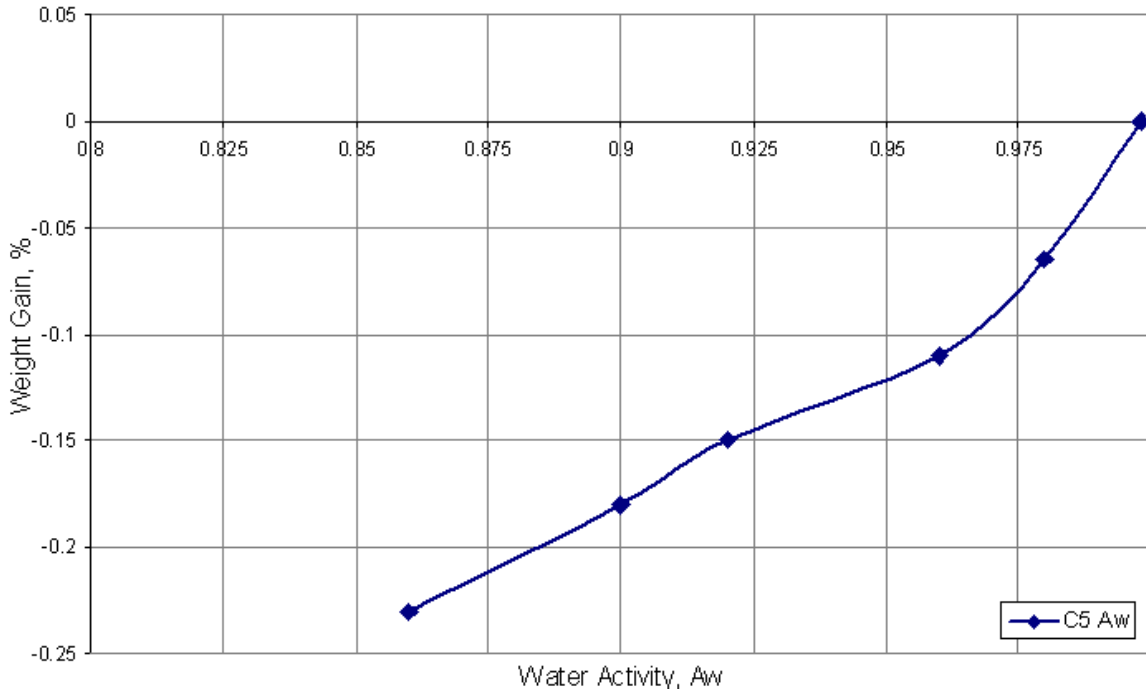


Figure 2.3: Native water activity of C5 shale

2.3 Gulf of Mexico Shale (GOM)

The GOM samples obtained from Newpark Drilling Fluids were prepared and stabilized over seven days using humidity controlled desiccators. Weight differences were taken before and after stabilization. As seen in Figure 2.4, the water activity of the shale is between 0.96 and 0.97. For convenience, it was decided to store the GOM shale in a previously developed 0.98 A_w desiccator.

Table 2.3: Native water activity data of GOM shale.

A_w	0.86	0.92	0.98
Weight1	39.755	41.5	37.33
Weight2	39.36	41.27	37.45
diff	-0.395	-0.23	0.12
%	-0.0099	-0.0055	0.0032

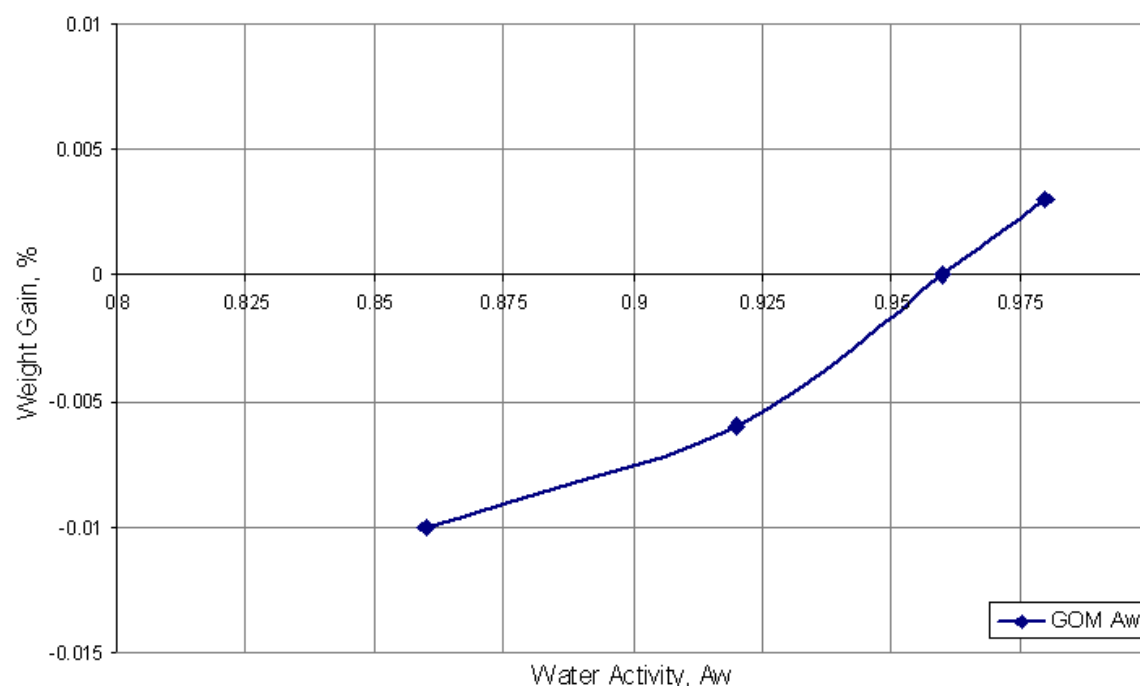


Figure 2.4: Native water activity of GOM shale

Chapter 3

Field Muds and Nanoparticle Properties

3.1 Field Mud Properties

Four different field muds were used to study the effect of NP's in contact with Atoka and GOM shales. Properties of each field mud before and after nanoparticle addition are presented in Tables 3.1 and 3.2. Muds were preserved from fermentation by adding 0.5 ppb X Cide 102 (Microbiocide) every week. Nyacol 9711 type nanoparticles were used for these mixtures since it is stable in high temperature and it does not produce flocculation when mixed with muds.

Table 3.1: Field muds properties.

Mud Properties	Newpark	Newpark	MISwaco	MISwaco
	Mud A	Mud B	Mud C	Mud D
Density, lb/gal	12	11.6	9.3	9.8
PV @ 80 F, cP	18	20	28	11
YP @ 80 F, lb/100ft ²	4	11	36	9
Solids Content, % by Volume	19.5	18.5	18.5	11
Water Content, % by Volume	77	79	79	88
Other Content, % by Volume	3.5	2.5	2.5	1
MBT, ppb Bentonite eq.	42.5	40	3.5	26.25
pH	8.7	11.4	9.4	11.4
Chlorides, mg/L	1900	65000	28000	320
LignoSulfonate Concentration, lb/bbl	100			
Water activity	1	0.93	0.98	1

Table 3.2: Properties of the field muds modified with Nyacol 9711 NP.

Mud-NP Mixture Properties	Nyacol 9711	Nyacol 9711	Nyacol 9711	Nyacol 9711
	Mud A+NP	Mud B+NP	Mud C+NP	Mud D+NP
PV @ 80 F, cP	8	10	19	6
YP @ 80 F, lb/100ft ²	1	5	19	2
Total solid vol %	22.5	21.5	21.2	15.5
NP wt %	10	10	10	10
NP vol %	8.3	7.8	6.9	7.1
pH	9	11	9	11

3.2 Nanoparticle Properties

A particle that has at least one dimension less than 100 nm is referred as a nanoparticle (NP). Nanotechnology refers to measurements in the scale of 1-100 nm. These materials have been applied in optical, electronic and biomedical sciences.

Two commercial nanoparticle companies provided us samples of silica nanoparticles: Nyacol and 3M. Both companies have 5 and 20 nm silica particles with different concentrations. The properties in our nanoparticle inventory are listed in Table 3.3. The effect of the salt concentration on NP stability was investigated with preliminary tests. 10 ml samples from each NP dispersion were taken and mixed with increasing salt concentrations and heated up until precipitation was observed. As seen in Table 3.3, the precipitation temperature is reduced with increasing salt concentration for both 3Ms and Nyacol's NP.

Table 3.3: Precipitation temperatures of NP dispersions.

Nanoparticle type	Precipitation Temperatures, F	Salt %wt
3M, 5nm, 17 wt %	180	2.4
3M, 5nm, 17 wt %	160	4
3M, 20 nm, 40 wt %	125	4
Nyacol Nexsil20A, 20 nm, 30 wt %	160	0.9
Nyacol Nexsil20A, 20 nm, 30 wt %	145	4
Nyacol Nexsil5, 5 nm, 15 wt %	160	4
Nyacol DP9711, 20 nm, 40 wt %	170	4

Filtration tests were first performed using 3M's 20 nm nanoparticle dispersions. Next, Nyacol DP9711 product was used. Nyacol DP9711 nanoparticles were more compatible with field muds than the 3M nanoparticles and Nyacol DP9711 was used for all field mud testing with both Atoka and GOM shales.

Chapter 4

Problem Statement, Test Procedure and Data Evaluation

4.1 Problem Statement

It is postulated herein that it is possible to reduce the permeability of shales by plugging their pore throats and their pores thereby building external and internal mudcakes.

Pore throat size can be determined by using a non-wetting fluid and the capillary pressure equation³. In Equation 4.1, P_c is the capillary pressure, σ is the interfacial tension between the non-wetting fluid and the water, θ is the contact angle and r is the pore throat radius.

$$P_c = \frac{2\sigma \cos(\theta)}{r} \dots\dots\dots(4.1)$$

The average pore throat sizes of shales range from 10 to 30 nanometers³. Compared to shale pore throat sizes, conventional drilling fluid additives, such as bentonite and barite, have much larger particle diameters, in the range of 0.1 to 100 micron (Figure 4.1).

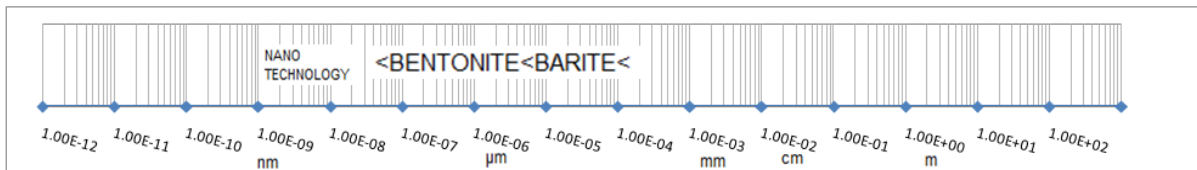


Figure 4.1: Particle Size Scale

Abrams ⁴ proposed that in order to form bridges, particle size should not be larger than one third of the pore throat size. This implies a particle size between 3 and 10 nm for typical shales. It is also stated by Abrams that for particles to achieve plugging, they should be at least 5% by volume of the drilling fluid. In conclusion, if the drilling fluid particles are slightly smaller than the pore throat size, they can invade into the shale, plug the pore throats and built an internal mudcake. This reduces the shale's permeability, and slows down water invasion.

4.2 Test Procedure

The test equipment used consists of a stainless steel test cell, a drilling fluid storage cylinder, flow lines, pressure transducers, manual pump for applying bottom pressure, a syringe injection pump for applying upstream pressure, a nitrogen cylinder, and a pressure recorder. As shown in Figure 4.2, the cell has a top sealing chamber, which has an inlet and outlet flow channel and a bottom chamber which has one pressure communication channel. These parts are assembled together using locking bolts and with O-rings that seal the top and bottom of the test specimen. The pressurized syringe pump regulates the flow rate of the fluid from the drilling fluid storage cylinder to the upstream chamber. The nitrogen gas cylinder provides the pressure for the control of back pressure on the drilling fluid outlet and a manual pump provides a hydraulic pressure of synthetic sea water to the bottom of the cell. Pressure transducers connected to the top and bottom lines send signals to the pressure recorders.

(Reference 3). Pressure difference at the beginning of the test is controlled by pumps both at the bottom and top of the shale. Total differential pressure applied to the shale during the test is the sum of Osmotic and Hydraulic pressure differences. Total differential pressure is explained with an example below.

As shown in Figure 4.3, at the beginning of the test, the top pressure is set at 300 psi and bottom pressure is set to 50 psi. Water activity of the top fluid is 1.0, water activity of the shale sample is 0.98, and water activity of the bottom fluid (synthetic sea water) is 0.98. The total differential pressure is calculated as shown below.

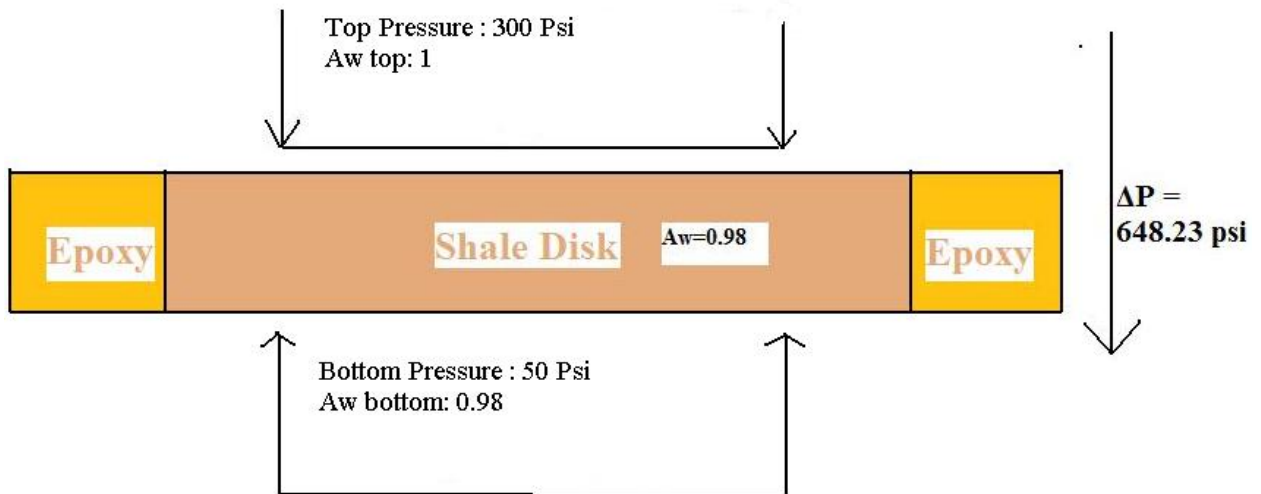


Figure 4.3: Differential pressure example

The calculation of osmotic pressure Π potential:

$$\Pi = 4.7 * \frac{RT}{V} \ln\left(\frac{A_w^{top}}{A_w^{bottom}}\right), psi \dots\dots\dots (4.2)$$

R = Universal gas constant ($8.21 * 10^{-5} \text{ m}^3 \text{ atm} / \text{Kmol}$)

T = Temperature ($297 \text{ }^{\circ}\text{K}$)

V = Partial molar volume of water ($18 \text{ cm}^3 / \text{mol}$)

A_w^{top} = Water activity of the top fluid (1.00)

A_w^{bottom} = Water activity of the bottom fluid (0.98)

$$\Pi = 398 psi$$

The calculation of the hydraulic pressure potential:

$$P_{top} - P_{bottom} = 300 - 50 = 250 psi$$

Total differential pressure potential = Hydraulic pressure + Osmotic Pressure

$$\Delta P = 398.23 + 250 = 648 psi$$

Data are evaluated using two techniques; by a) fluid invasion comparison between two separate tests and b) absolute permeability.

a. Fluid invasion comparison technique.

In this technique, the fractional reduction in top and bottom pressures at the end of Tests 1 and 2 are calculated using equations 4.3 and 4.4 respectively.

$$\frac{\Delta P_{i1} - \Delta P_{f1}}{\Delta P_{i1}} \dots\dots\dots(4.3)$$

where;

ΔP_{i1} : Initial hydraulic differential pressure in example 1 (psi)

ΔP_{f1} : Final hydraulic differential pressure in example 1 (psi)

$$\frac{\Delta P_{i2} - \Delta P_{f2}}{\Delta P_{i2}} \dots\dots\dots(4.4)$$

where;

ΔP_{i2} : Initial hydraulic differential pressure in example 2 (psi)

ΔP_{f2} : Final hydraulic differential pressure in example 2 (psi)

Then the reduction in fluid invasion by comparison, is obtained by using Equation 4.5

Reduction in fluid invasion in two tests is formulated as:

$$\frac{\frac{\Delta P_{i1} - \Delta P_{f1}}{\Delta P_{i1}} - \frac{\Delta P_{i2} - \Delta P_{f2}}{\Delta P_{i2}}}{\frac{\Delta P_{i1} - \Delta P_{f1}}{\Delta P_{i1}}} \dots\dots\dots(4.5)$$

As an example, refer to Figures 4.4 for fluid 1 and Figure 4.5 for fluid 2, inserting these values into Equation 4.5 we have,

$$\frac{\frac{240 - 60}{240} - \frac{260 - 200}{260}}{\frac{240 - 60}{240}} = 0.69 = 69\% \text{ reduction in fluid invasion.}$$

As seen in Figure 4.4, the initial differential pressure is 240 psi and final differential pressure is 60 psi. Similarly, as seen in Figure 4.5, the initial differential pressure is 260 psi and final differential pressure is 200 psi.

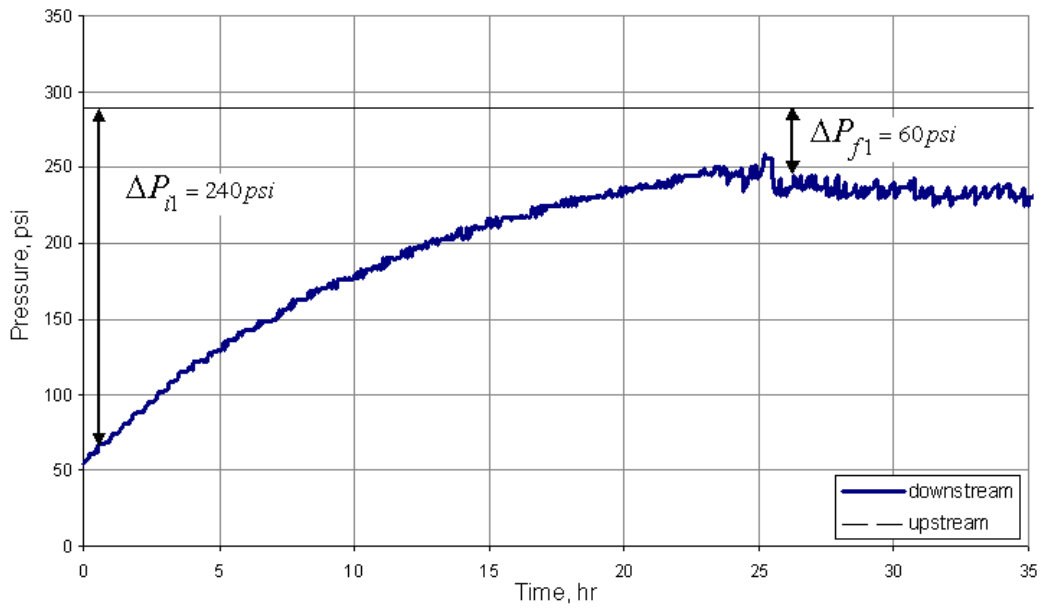


Figure 4.4: Example 1 test result

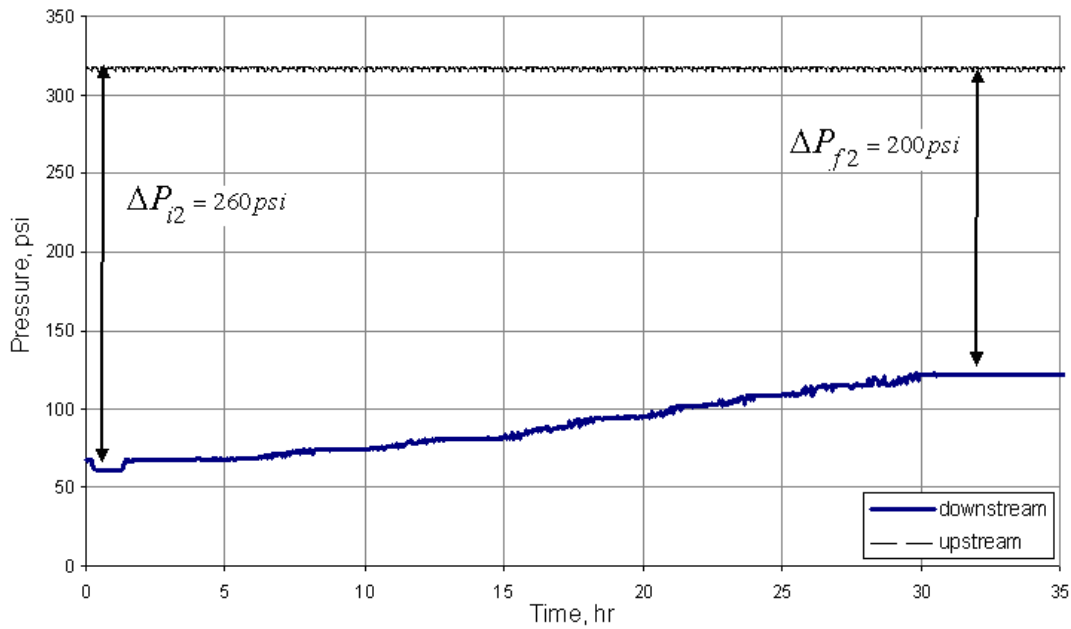


Figure 4.5: Example 2 test result

b. Absolute permeability technique

The second data evaluation type that was used in this study is permeability reduction. To explain how permeability is calculated Figure 4.6 is used as an example.

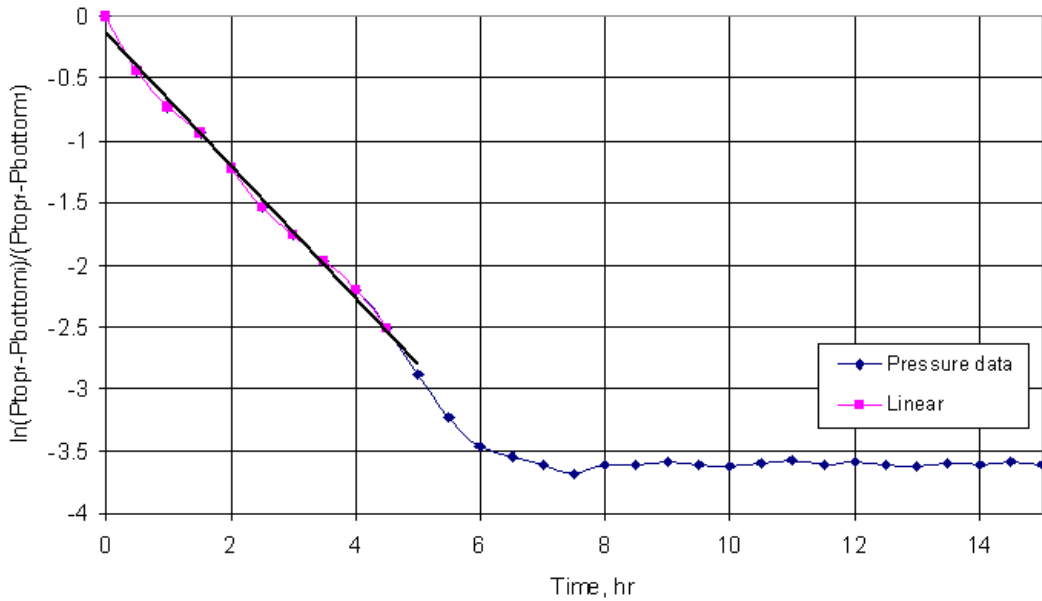


Figure 4.6: Example 3 permeability calculation plot

Permeability Calculation is based on the work of Al-Bazali et. al. ³:

$$k = \frac{-m\mu CVh}{A} \text{ cm}^2 \dots\dots\dots(4.6)$$

where;

k: Permeability (cm²)

m: Slope/3600 of the linear portion of curve in Figure 4.6

μ: Viscosity (psi.second)

C: Compressibility, psi⁻¹

V: Volume (cm³)

A: Area, cm² (Surface area of the shale sample exposed to the upstream flow)

Chapter 5

Preliminary Testing

5.1 Swelling Test

The first study was performed using granite. Tests showed that the NP dispersion could easily pass through the sample of granite. The second study was performed to see if a 1.3 nano darcy mud cake could be plugged with nanoparticles. Using past filtration data ⁵ as a guide this cake was made using a mud that contained 10 ppb bentonite and 1 ppb CMC. Again, the NP dispersion easily passed through the mud cake.

While waiting for shale equilibrium, a third study was performed using two 1 inch by ½ inch by ½ inch pieces of C5 shale and a swell meter. In these tests, one sample was immersed in water and second sample was immersed in a 41 wt % dispersion of 20 nm particles. As shown in Figure 5.1, after about 1080 minutes, the C5 shale that was immersed in the water had experienced about 10.8 % swelling and the NP dispersion experienced only 6.4 % swelling. In other words, swelling was reduced by 41 % by using the NP dispersion.

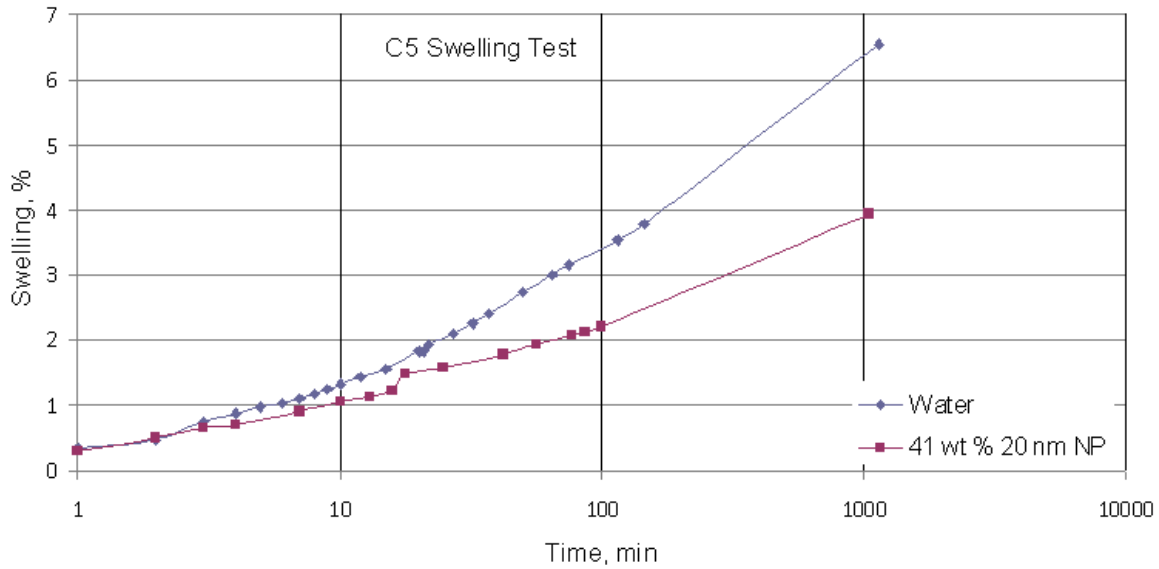


Figure 5.1: C5 Shale swelling test performed with fresh water and NP dispersion.

5.2 Multi-step Tests

In Test 5.1, (Figure 5.2), a three-step procedure was followed. Using the flow equipment described in Appendix A, first, low salinity brine (sea water) was flowed across the shale sample (step 5.1.a) and it easily penetrated the shale completely in about 25 hours. The test was continued by reducing the bottom pressure of the shale and again the sea water easily penetrated the shale (see 25 to 34 hours of Figure 5.2). Then in the third step (5.1.c) the NP dispersion flowed across the same shale sample and complete shale plugging occurred in only 5 hours (see 34 to 39 hours). Again we see that the NP dispersion can reduce flow into the shale. As shown in Figure 5.2, 3M’s 20 nm 41 wt % silica NP dispersion reduced the fluid penetration by 95 % in 6 hours compared to the brine. The test configuration is shown in Table 5.1.

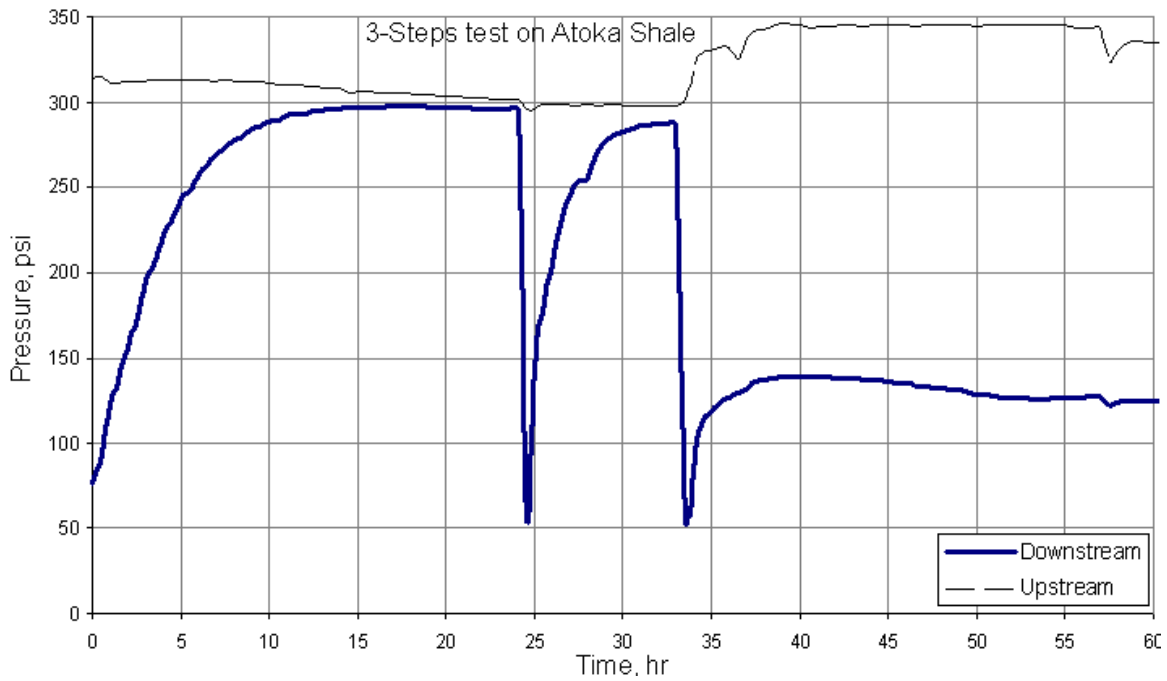


Figure 5.2: Three steps test in contact with Atoka shale

Table 5.1: 3M two steps test in contact with Atoka shale

Test	5.1.a	5.1.b	5.1.c
Date	4/3-5/2008	4/3-5/2008	4/3-5/2008
Shale	Atoka	Atoka	Atoka
Brand	3M	3M	3M
Top Fluid	Brine	Brine	NP
NP wt%	0	0	41
NP Size (nm)	-	-	20
Bottom Fluid	Brine	Brine	Brine
Aw top	0.98	0.98	0.98
Aw Bottom	0.98	0.98	0.98
Aw shale	0.98	0.98	0.98
Top Pres. (Psi)	325	325	350
Bottom Pres. (Psi)	75	50	50

Test 5.2 was performed by following a two-step procedure to see if a high concentration of NP would completely plug the pore throats. In the first step, (5.2.a), (0-28 hours), 3M's 20 nm particle dispersion was used, and the plugging occurred in two hours. In the second step (5.2.b), (28-55 hours), brine was used without NP and the bottom pressure built up to 250 psi differential pressure after 25 hours, which means that there was a very little penetration through the shale. As shown in Figures 5.2 and 5.3, 3M's 20 nm 41 wt % silica NP dispersion reduced the fluid penetration by 98 % in 6 hours compared to brine. This result shows that the NP dispersion had permanently plugged the shale. The test configuration is shown in Table 5.2.

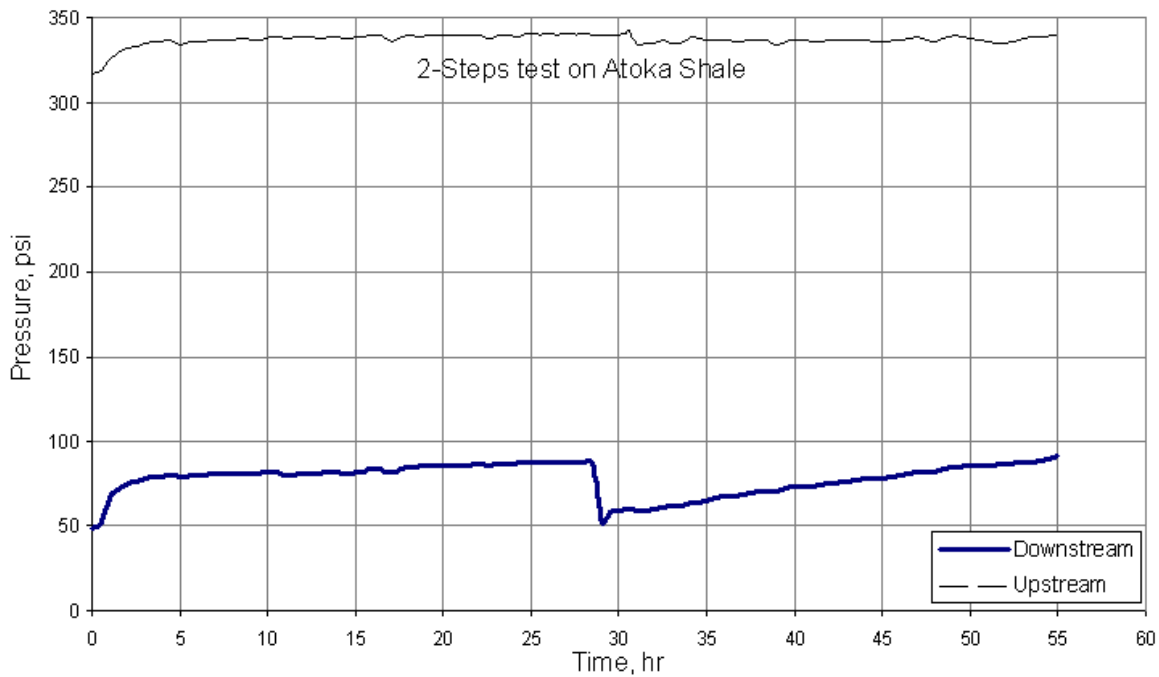


Figure 5.3: Two step test with and without NP

Table 5.2: 3M 20 nm two step test in contact with Atoka shale

Test	5.2.a	5.2.b
Date	4/6-9/2008	4/6-9/2008
Shale	Atoka	Atoka
Brand	3M	3M
Top Fluid	NP	Brine
NP wt%	41	0
NP Size (nm)	20	-
Bottom Fluid	Brine	Brine
Aw top	0.98	0.98
Aw Bottom	0.98	0.98
Aw shale	0.98	0.98
Top Pres. (Psi)	340	340
Bottom Pres. (Psi)	50	50

Test 5.3 was performed to see how a NP dispersion works in another type of shale, the C5. The test consisted of three-steps as shown in Figure 5.4. In the first step (5.3.a), (0-6 hours), negative osmotic pressure was applied to the sample with a lower water activity brine ($a_w = 0.85$). The bottom pressure built up to the top pressure in 6 hours. The second step (5.3.b), (6-10 hours) was performed with a brine solution which had a 0,98 A_w , the same A_w as the sample and the bottom fluid. The bottom pressure built up to the top pressure in 3 hours. In the third step (5.3.c), a 20 nm 41w% NP dispersion was used as a top fluid and pressure built up to a differential pressure of 150 psi after 7 hours. As shown in Figure 5.4, 3M's 20 nm 41 wt % silica NP dispersion reduced the fluid penetration by 96 % in 6 hours compared to brine. The test configuration is shown in Table 5.3.

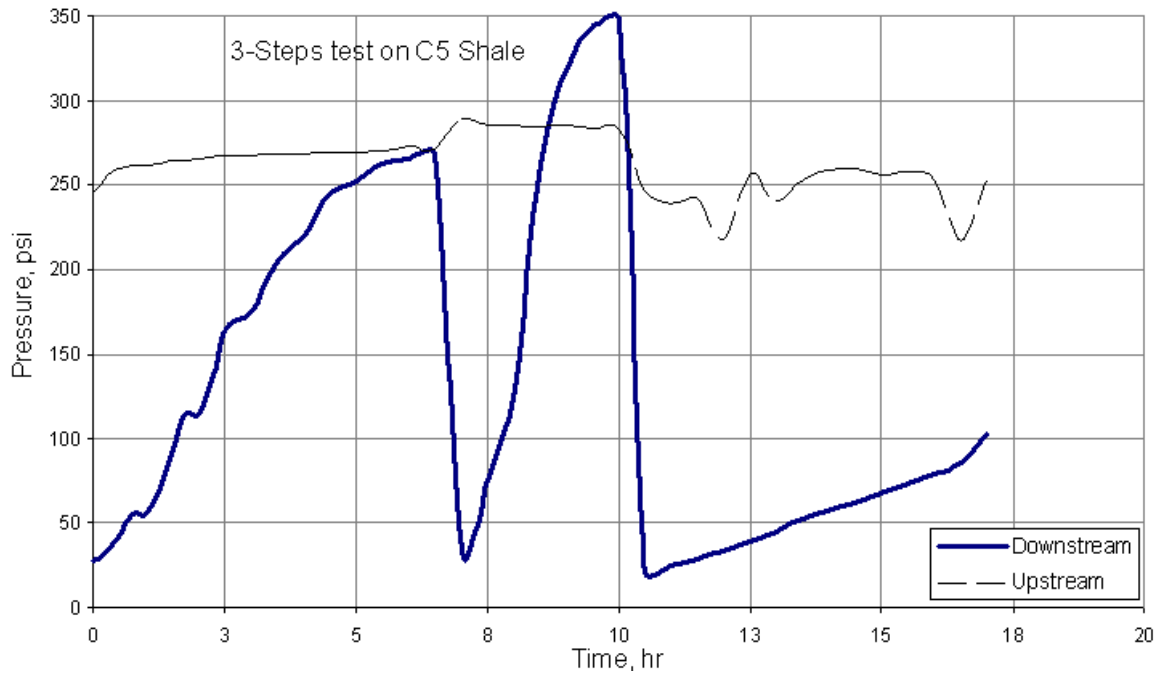


Figure 5.4: Three step test with C5 shale without and with NP

Table 5.3: 3M 20 nm three step test on C5 shale

Test	5.3.a	5.3.b	5.3.c
Date	4/17/2008	4/17/2008	4/17/2008
Shale	C5	C5	C5
Brand	-	-	3M
Top Fluid	Brine	Brine	NP
NP wt%	0	0	41
NP Size (nm)	-	-	20
Bottom Fluid	Brine	Brine	Brine
Aw top	0.98	0.98	0.98
Aw Bottom	0.85	0.98	0.98
Aw shale	0.98	0.98	0.98
Top Pres. (Psi)	250	250	250
Bottom Pres. (Psi)	40	40	40

5.3 Nanoparticle Concentration Tests

Test 5.4 was performed to investigate if a reduced weight percentage (29 wt %) of NP dispersion would work as well as 41 wt %. As seen in Figure 5.5, the bottom pressure did not build up at all. Complete plugging was achieved. The test configuration is shown in Table 5.4.

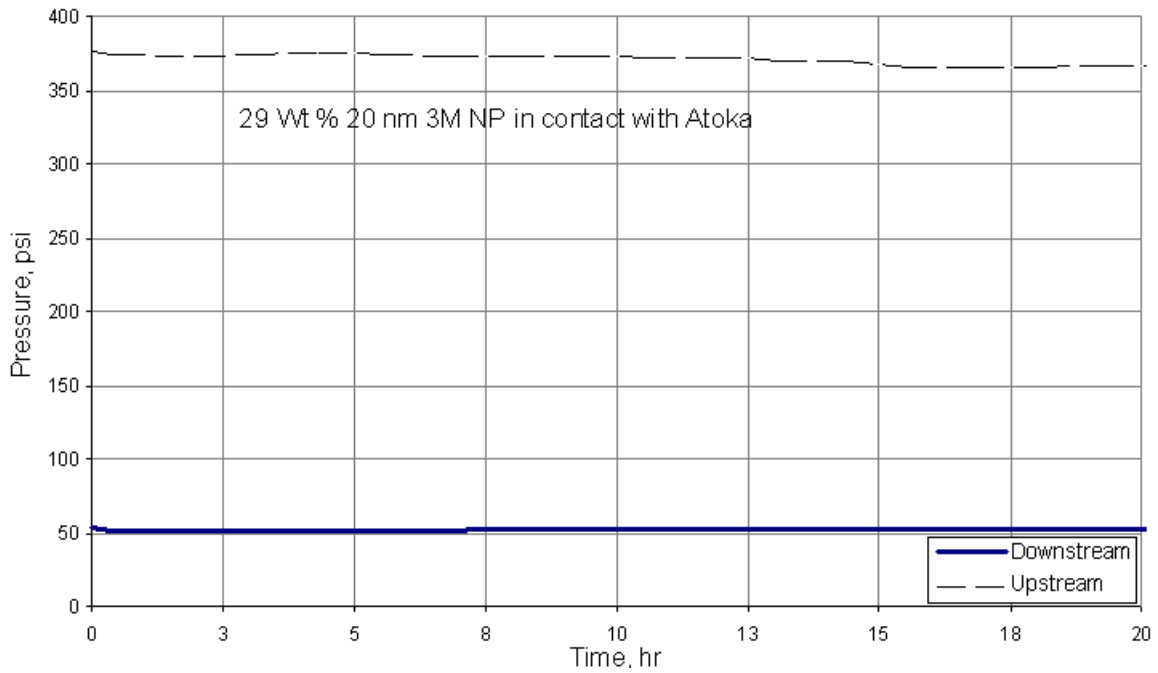


Figure 5.5: Results of the Atoka/ 29 wt % NP dispersion test.

Table 5.4: 3M 20 nm 29 wt % test in contact with Atoka shale

Test	5.4
Date	5/2-3/2008
Shale	Atoka
Brand	3M
Top Fluid	NP
NP wt%	29
NP Size (nm)	20
Bottom Fluid	Brine
Aw top	0.98
Aw Bottom	0.98
Aw shale	0.98
Top Pres. (Psi)	350
Bottom Pres. (Psi)	50

Test 5.5 was performed under the same conditions as the seventh test, except for the NP dispersion weight percentage. The test was performed with 5 wt % NP dispersion and resulted in a bottom pressure buildup of 100 psi differential in 35 hours. As shown in Figure 5.6, 3M 5 wt% NP dispersion concentration is not as effective as 10 wt %. It can be concluded that a 10 wt % is the minimum concentration for penetration reduction. The test configuration is shown in Table 5.5.

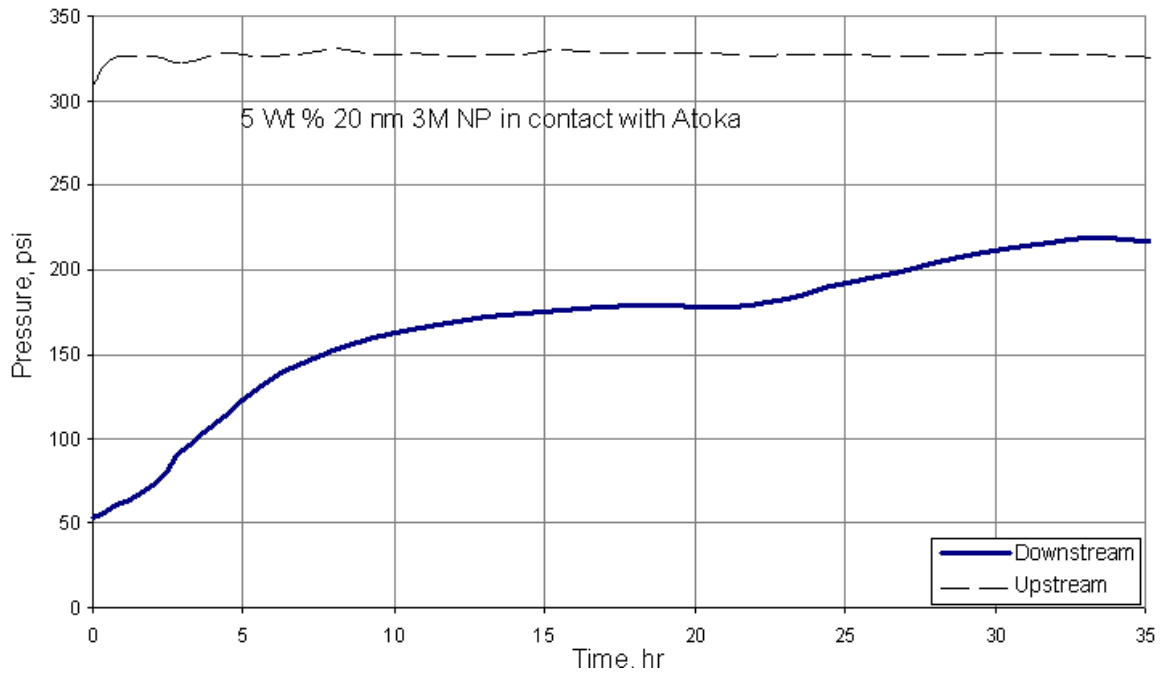


Figure 5.6: Results of the test which was performed with 3M 20 nm 5 wt % NP dispersion

Table 5.5: 3M 20 nm 5 wt % test in contact with Atoka shale

Test	5.5
Date	5/13-14/2008
Shale	Atoka
Brand	3M
Top Fluid	NP
NP wt%	5
NP Size (nm)	20
Bottom Fluid	Brine
Aw top	0.98
Aw Bottom	0.98
Aw shale	0.98
Top Pres. (Psi)	325
Bottom Pres. (Psi)	50

Test 5.6 was performed under the same conditions as the eighth test except for the NP dispersion weight percentage. The test was performed with 10 wt % NP dispersion and the bottom pressure stabilized at a 250 psi differential pressure in 8 hours as shown in Figure 5.7. The test configuration is shown in Table 5.6.

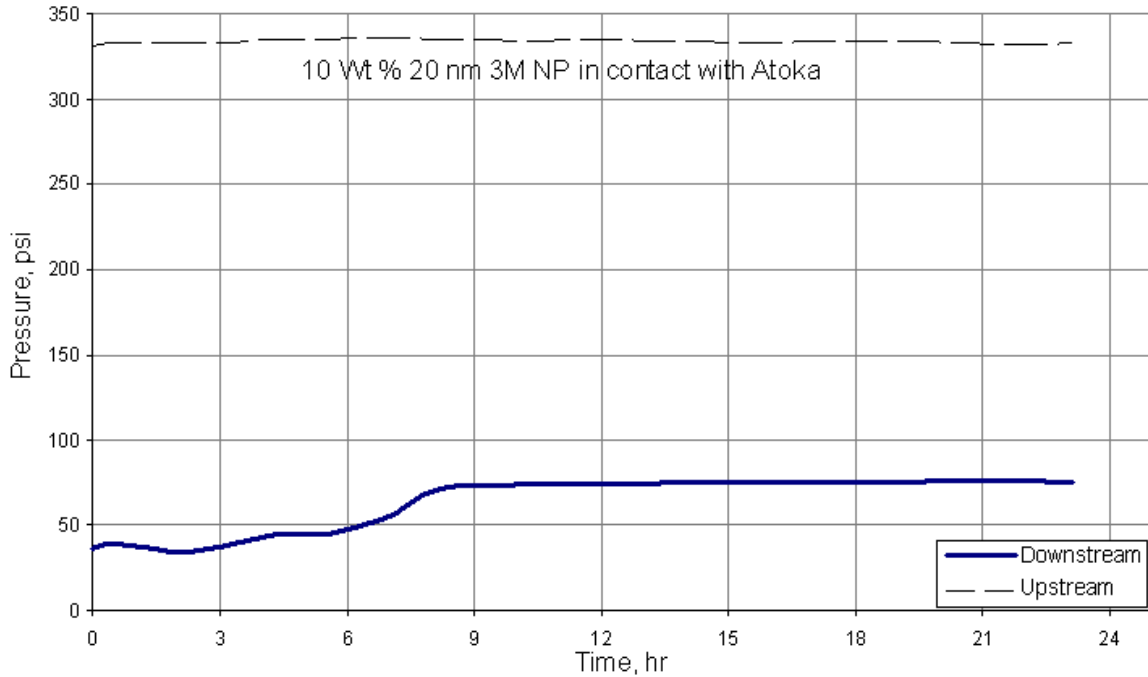


Figure 5.7: Results of the test which was performed with 10 w % NP dispersion.

Table 5.6: 3M 20 nm 10 wt % test in contact with Atoka shale

Test	5.6
Shale	Atoka
Brand	3M
Top Fluid	NP
NP wt%	10
NP Size (nm)	20
Bottom Fluid	Brine
Aw top	0.98
Aw Bottom	0.98
Aw shale	0.98
Top Pres. (Psi)	325
Bottom Pres. (Psi)	40

As shown in Figure 5.8, silica nanoparticles reduce the fluid invasion into the shale compared to the brine. Another conclusion is that the minimum concentration required to reduce the fluid penetration is 10 wt % NP.

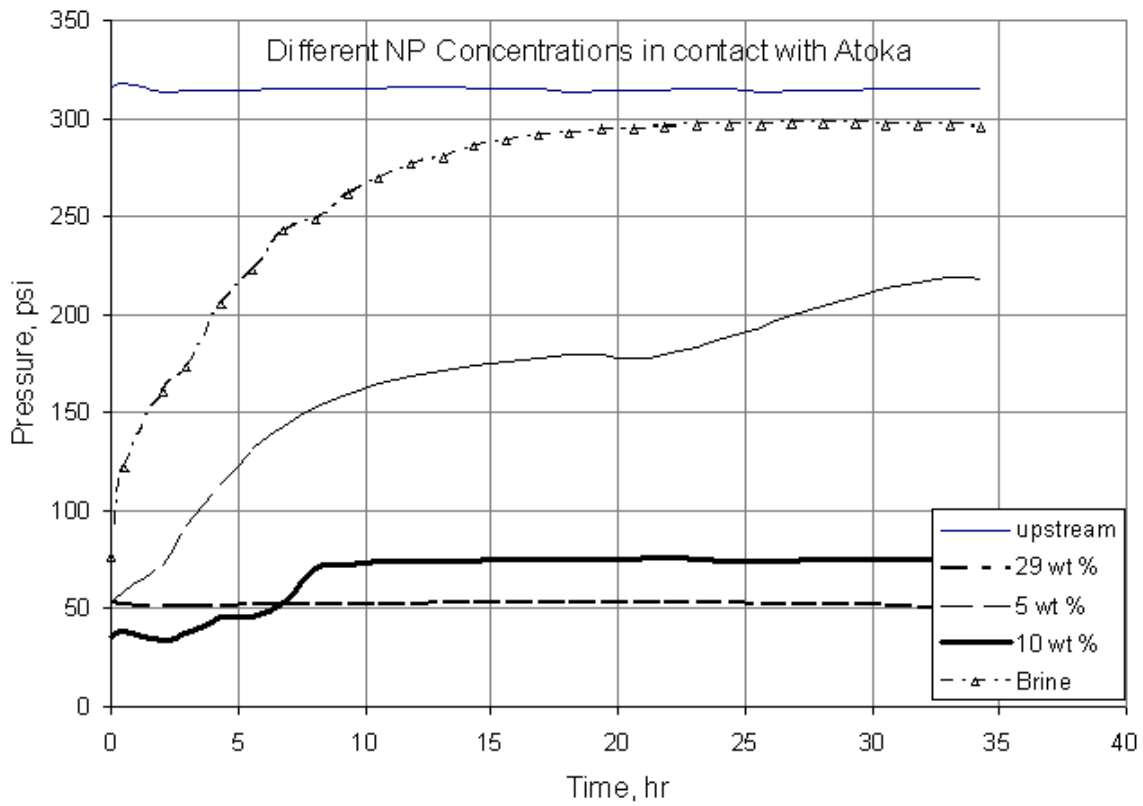


Figure 5.8: NP tests with different concentrations in contact with Atoka shale.

5.4 Scanning Electron Micrographs

The next study consisted of using Scanning Electron Micrographs to visualize the type of plugging that was taking place. Figures 5.9 to 5.11 were obtained using an Atoka shale sample that had been tested with 3M's 20 nm 29 w% silica NP dispersion.

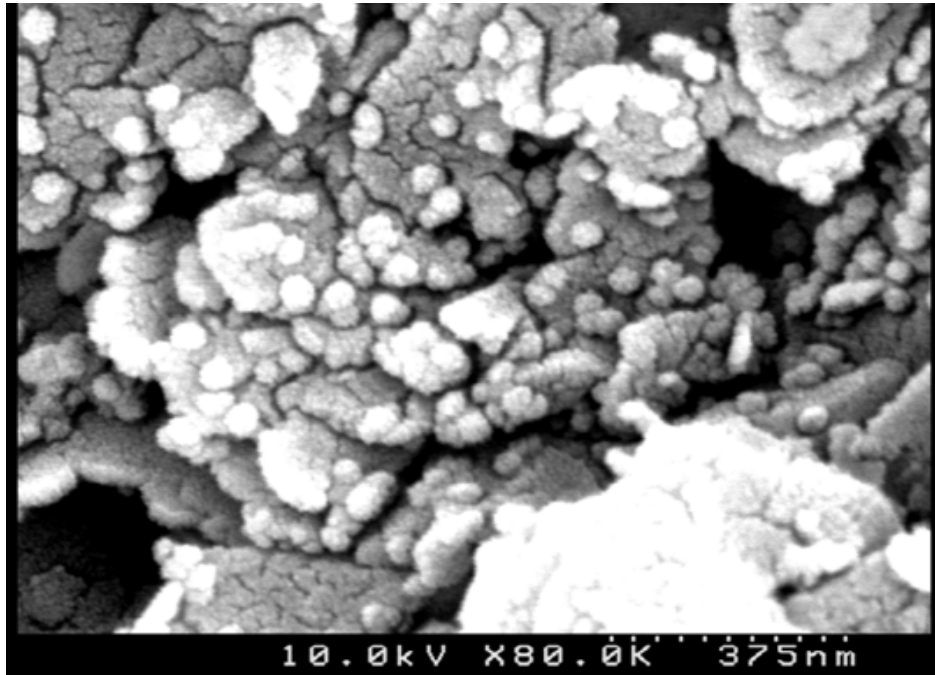


Figure 5.9: SEM of 20 nm particles in contact with Atoka shale. (Dotted scale is 375 nm)

In Figures 5.9 and 5.10, it is seen that Atoka shale has a wide range of pore throats and 20 nm particles could plug just the ones that fit that size. This result suggests that if a NP mixture which consists of different sized particles between 5-50 nm, more pores could be plugged. It is easily seen in the lower-center of Figure 5.11 that the group of 20 nm nanoparticles can plug one big sized pore throat.

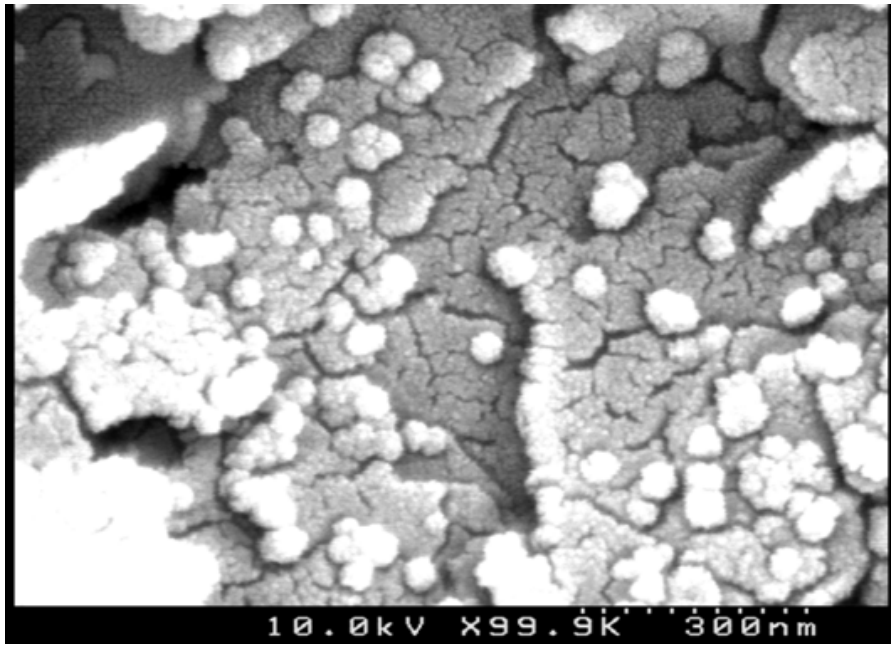


Figure 5.10: 20 nm silica NP in different scale

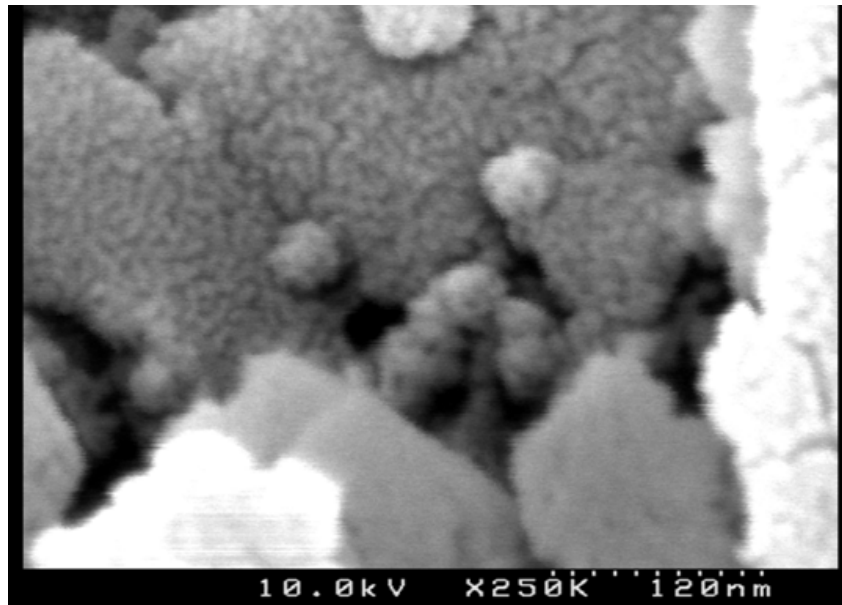


Figure 5.11: Group of particles plugged a pore throat

5.5 Nanoparticle Type and Size Tests

Test 5.7 was performed to investigate the effect of the Nyacol's 20 nm particles in contact with Atoka shale. This test is the first straight application of 20 nm Nyacol's silica NP dispersion. In this test a sample of Atoka shale was exposed to a 40 wt %, 20 nm NP dispersion. Table 5.7 shows the test condition. As seen in Figure 5.12, the bottom pressure built up in 17 hours at about 12 psi /hour, which is considered high. Nyacol's 20 nm particles did not plug the pores as well as 3M's 20 nm particles did in tests 5.2, 5.3, 5.4 and 5.6.

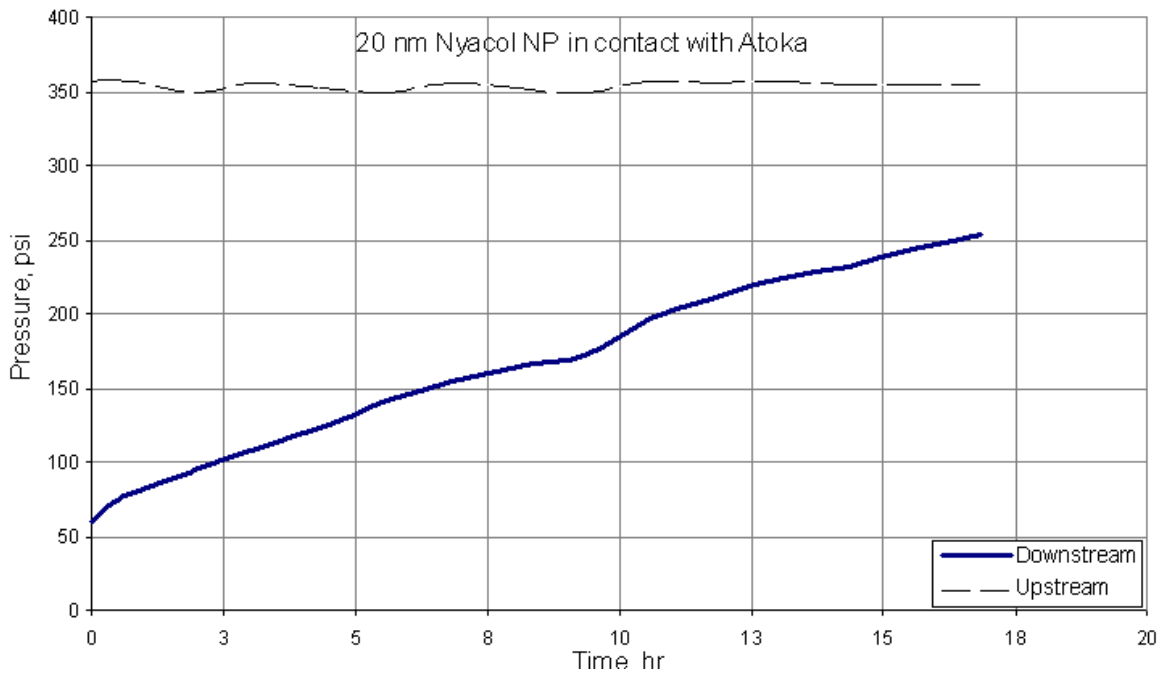


Figure 5.12. Results of the Test 5.7 which was performed with Nyacol 40 wt % 20 nm dispersion.

Table 5.7: Conditions in Test 5.7.

Test	5.7
Date	9/13/2008
Shale	Atoka
Brand	Nyacol
Top Fluid	NP
NP wt%	41
NP Size (nm)	20
Bottom Fluid	Brine
Aw top	1
Aw Bottom	0.98
Aw shale	0.98

Test 5.8 and 5.9 were performed to investigate the effect of the Nyacol's and 3M's 5nm particles in contact with Atoka shale. These tests are the first trials of 5nm particles. 3M's and Nyacol's 17 wt % and 15 wt %, 5 nm NP dispersions flowed across the surface of the Atoka shale sample. Test conditions are shown in Table 5.8. As seen in Figure 5.13, the bottom pressure built up to top pressure in 25 hours. 5nm particles did not plug the pores as much as 20 nm particles did.

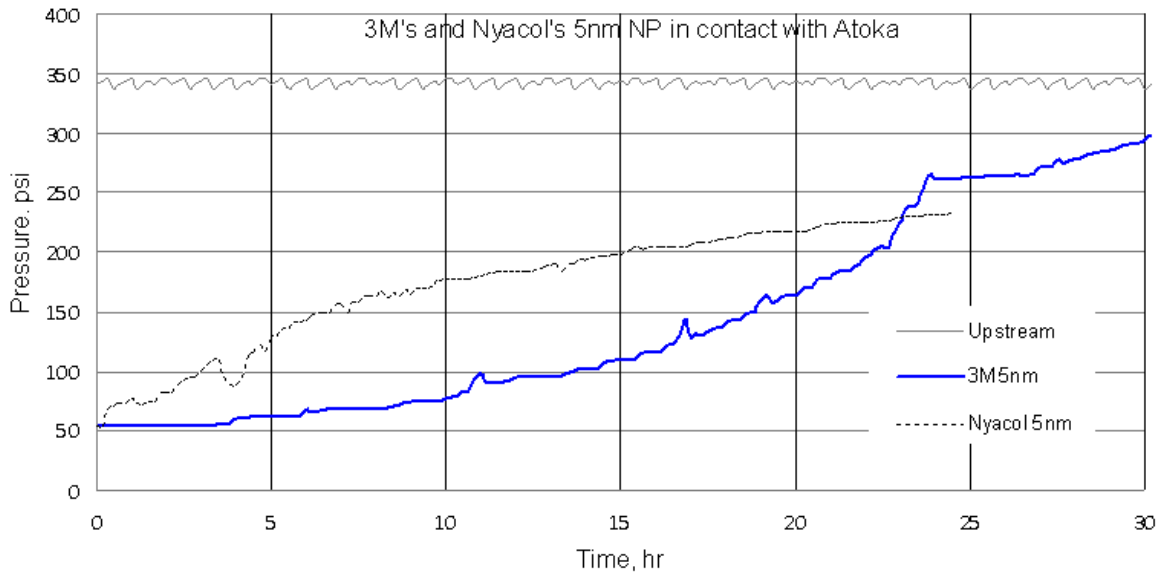


Figure 5.13. 3M's 17 wt % and Nyacol's 15 wt % 5 nm dispersions in contact with Atoka.

Table 5.8: Conditions in Test 5.8 and 5.9.

Test	5.8	5.9
Date	9/19/2008	9/20/2008
Shale	Atoka	Atoka
Brand	Nyacol	3M
Top Fluid	NP	NP
NP wt%	15	17.71
NP Size (nm)	5	5
Bottom Fluid	Brine	Brine
Aw top	0.98	0.98
Aw Bottom	0.98	0.98
Aw shale	0.98	0.98
Top Pres. (Psi)	340	340
Bottom Pres. (Psi)	55	55

Chapter 6

Field Mud Tests

6.1 Field Muds in contact with Atoka shale

Test 6.1 was performed to observe the performance of Mud A. Table 6.1 gives the test conditions. As seen in Figure 6.1, the bottom pressure stabilized at 60 psi differential pressure in 25 hours. Using the transient method discussed in Chapter 4 the permeability of the sample was determined to be 0.044 nd. The pressure drop of 15 psi in the last 8 hours of this test is believed to be result of temporary temperature change in the laboratory.

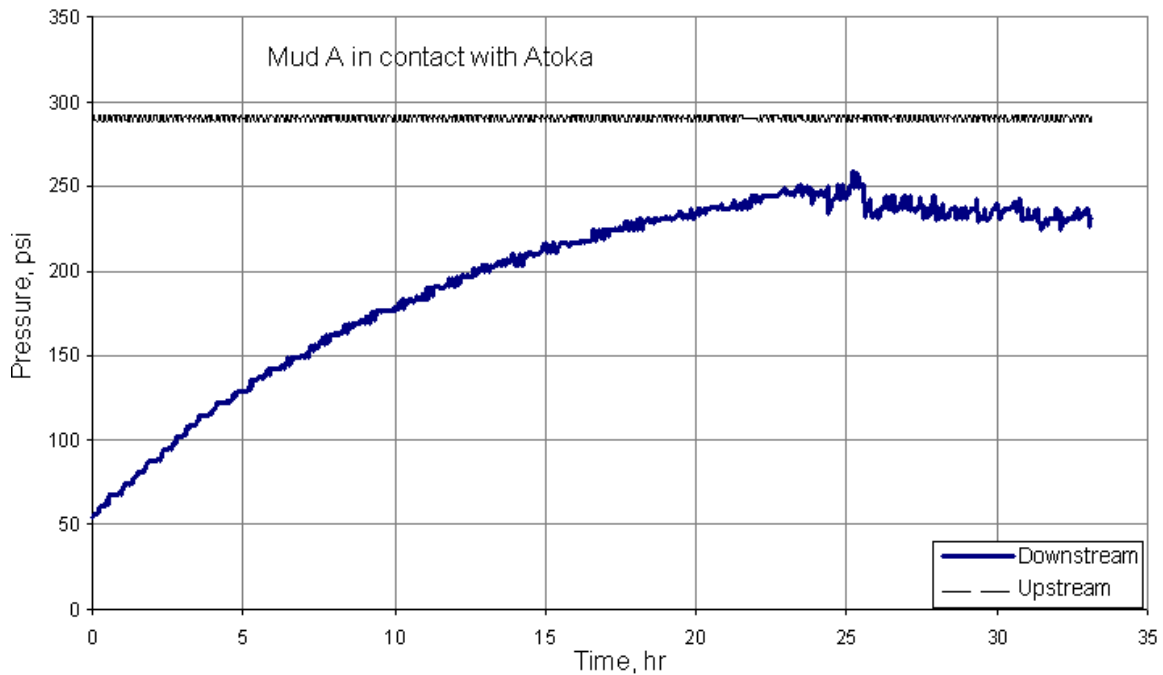


Figure 6.1: Results of Test 6.1 that was performed in contact with Atoka shale.

Table 6.1: Conditions for Test 6.1.

Test	6.1
Date	11/3/2008
Shale	Atoka
Top Fluid	Mud A
NP wt%	0
Bottom Fluid	Brine
Aw top	1
Aw Bottom	0.98
Aw shale	0.98
Top Pres. (Psi)	290
Bottom Pres. (Psi)	50
Result	Stabilized at 60 psi differential pressure in 25 hours with a permeability of 0.044 nd.

Test 6.2 was performed to observe the effect of the Nyacol nanoparticle dispersion on the performance of Mud A. Mud A, which was modified with 10 wt% Nyacol NP, was flowed across the Atoka shale sample. Table 6.2 shows the test conditions and Table 6.3 shows the mud composition. As shown in Figure 6.2 the bottom pressure stabilized at 170 psi differential pressure in 35 hours. As shown in Figure 6.3, adding Nyacol's silica NP dispersion to the Field Mud A reduced the fluid penetration by 72 % in 36 hours. Using the transient method discussed in Chapter 4 the permeability of the sample was determined to be 0.0038 nd.

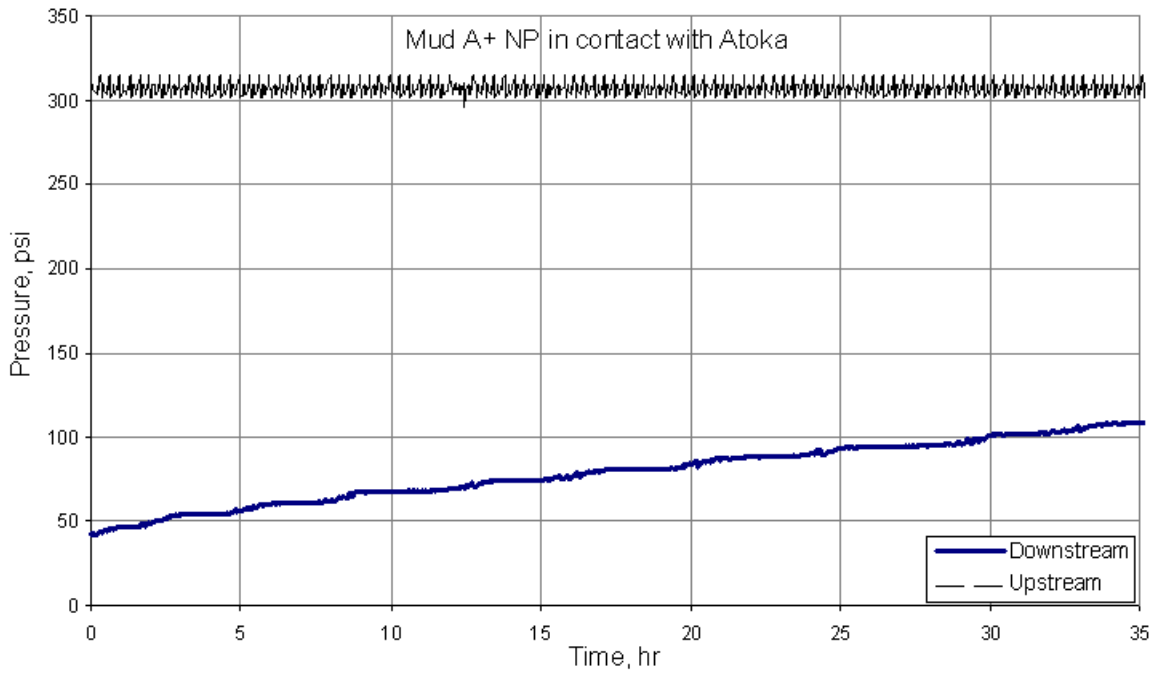


Figure 6.2: Results of Test 6.2 that was performed in contact with Atoka shale.

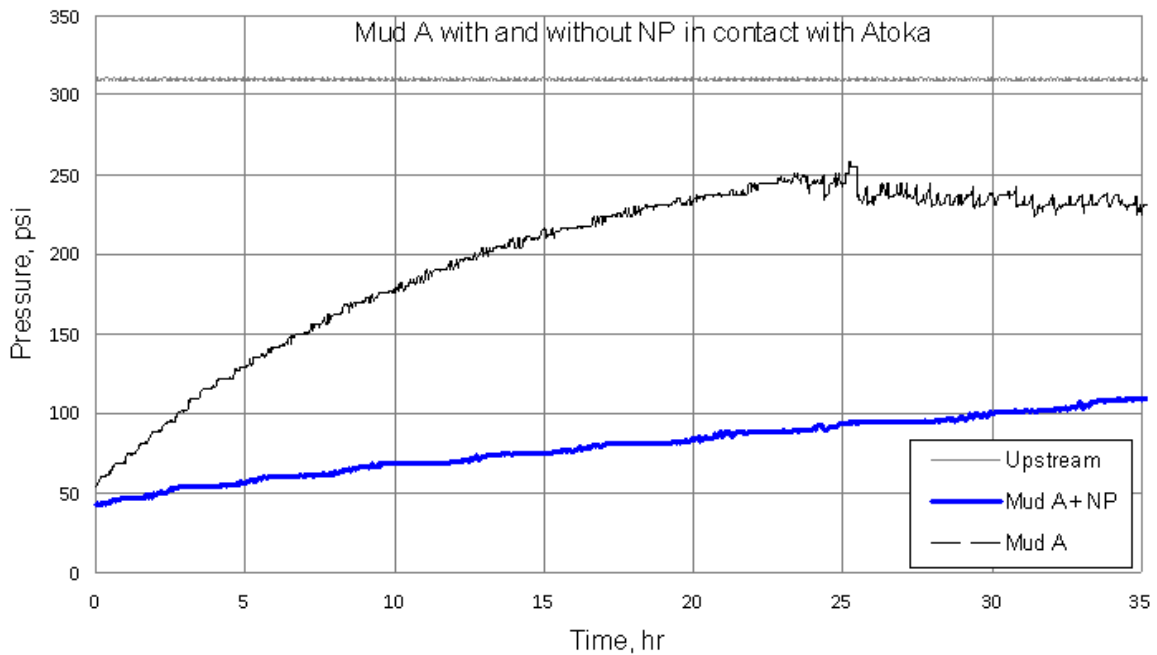


Figure 6.3: Comparison of Mud A with and without NP in contact with Atoka shale.

Table 6.2: Conditions for Test 6.2

Test	6.2
Date	11/18/2008
Shale	Atoka
Brand	Nyacol 9711
Top Fluid	Mud A +NP
NP wt%	10
NP Size (nm)	20
Bottom Fluid	Brine
Aw top	1
Aw Bottom	0.98
Aw shale	0.98
Top Pres. (Psi)	290
Bottom Pres. (Psi)	50
Result	Maintained 170 psi differential pressure for 35 hours with a permeability of 0.0038 nd.

Table 6.3: Composition in Test 6.2

Mud A+ NP	Volume, cc	Mass, gr
Mud solid	17.33	56.44
mud water	71.56	71.56
mud total	88.89	128.00
NP solid	10.13	16.80
NP sol. water	23.20	23.20
NP sol. total	33.33	40.00
Total Solid %	22.5%	43.6%
NP %	8.3%	10.0%

Test 6.3 was performed to observe the response of Mud B in contact with Atoka shale. Table 6.4 shows the test conditions. As seen in Figure 6.4, the bottom pressure stabilized at 180 psi differential pressure in 30 hours. Using the transient method discussed in Chapter 4 the permeability of the sample was determined to be 0.0047 nd.

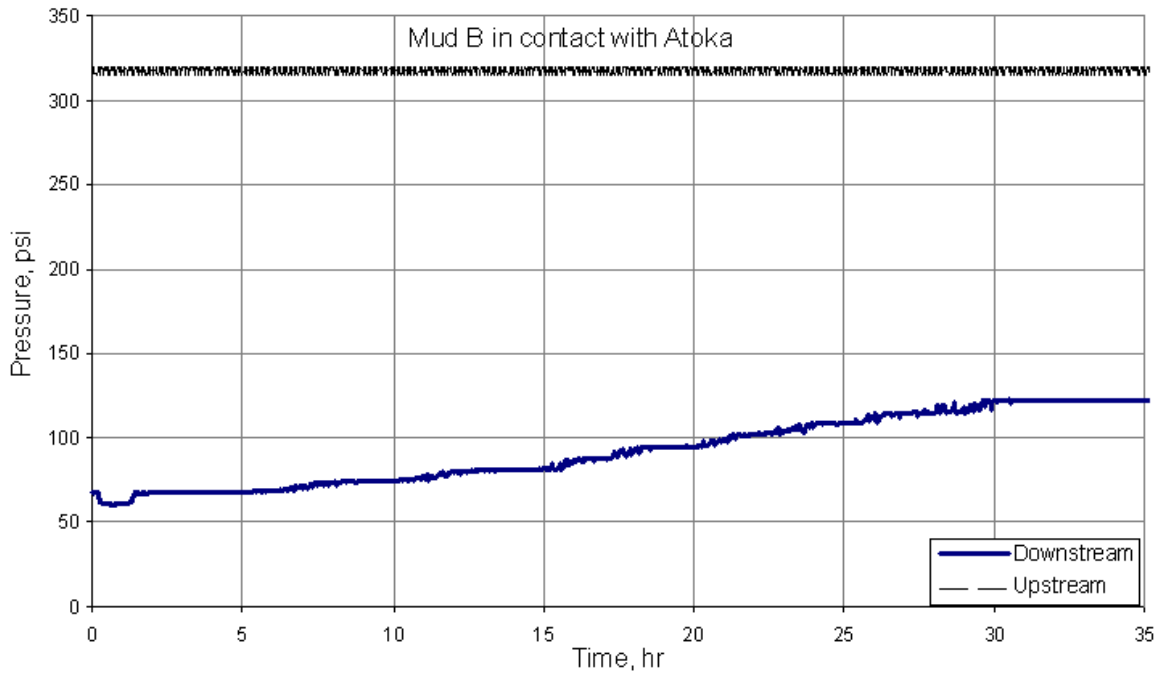


Figure 6.4: Results of Test 6.3 that was performed in contact with Atoka shale.

Table 6.4: Conditions for Test 6.3.

Test	6.3
Date	12/1/2008
Shale	Atoka
Top Fluid	Mud B
NP wt%	0
Bottom Fluid	Brine
Aw top	0.93
Aw Bottom	0.98
Aw shale	0.98
Top Pres. (Psi)	330
Bottom Pres. (Psi)	70
Result	Stabilized at 200 psi differential pressure in 30 hours with a permeability of 0.0047 nd.

Test 6.4 was performed to observe the effect of the Nyacol nanoparticle dispersion on the response of Mud B in contact with Atoka shale. Table 6.5 shows the test conditions and Table 6.6 shows the mud composition. Mud B, which was modified with 10 wt% Nyacol NP, was flowed across the Atoka shale sample. As seen in Figure 6.5, the bottom pressure stabilized at 210 psi differential pressure in 20 hours. As shown in Figure 6.6, adding Nyacol's silica NP dispersion to the Field Mud B reduced the fluid penetration by 16 % in 36 hours. Using the transient method discussed in Chapter 4 the permeability of the sample was determined to be 0.0058 nd.

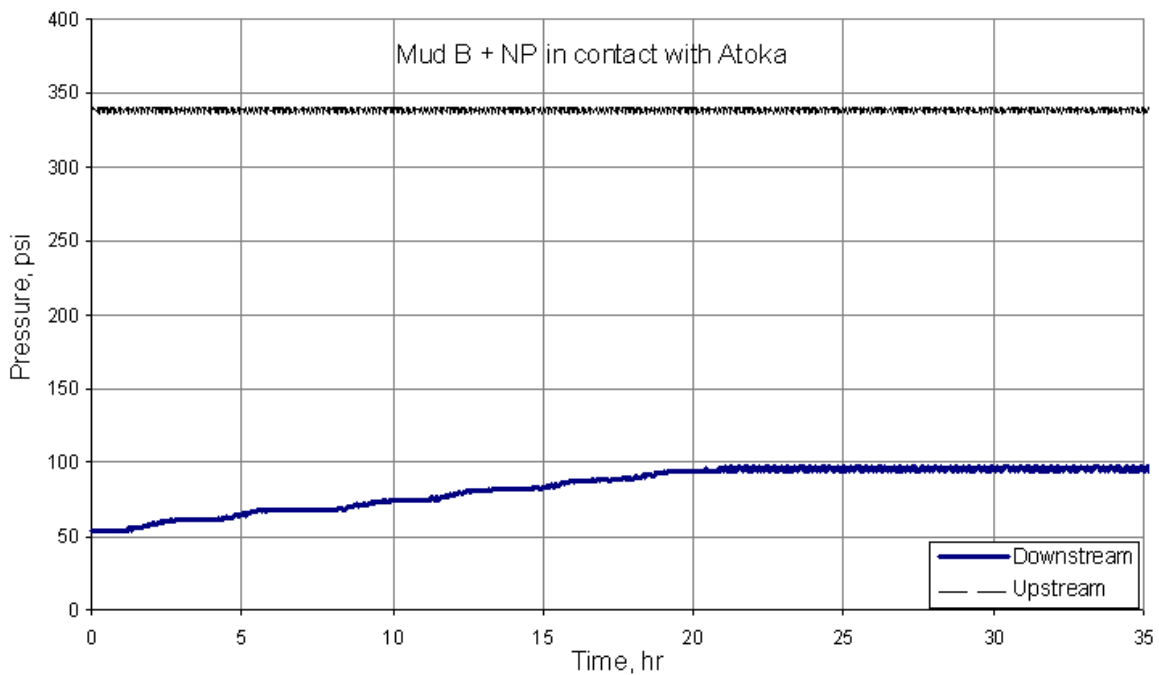


Figure 6.5: Results of Test 6.4 that was performed in contact with Atoka shale.

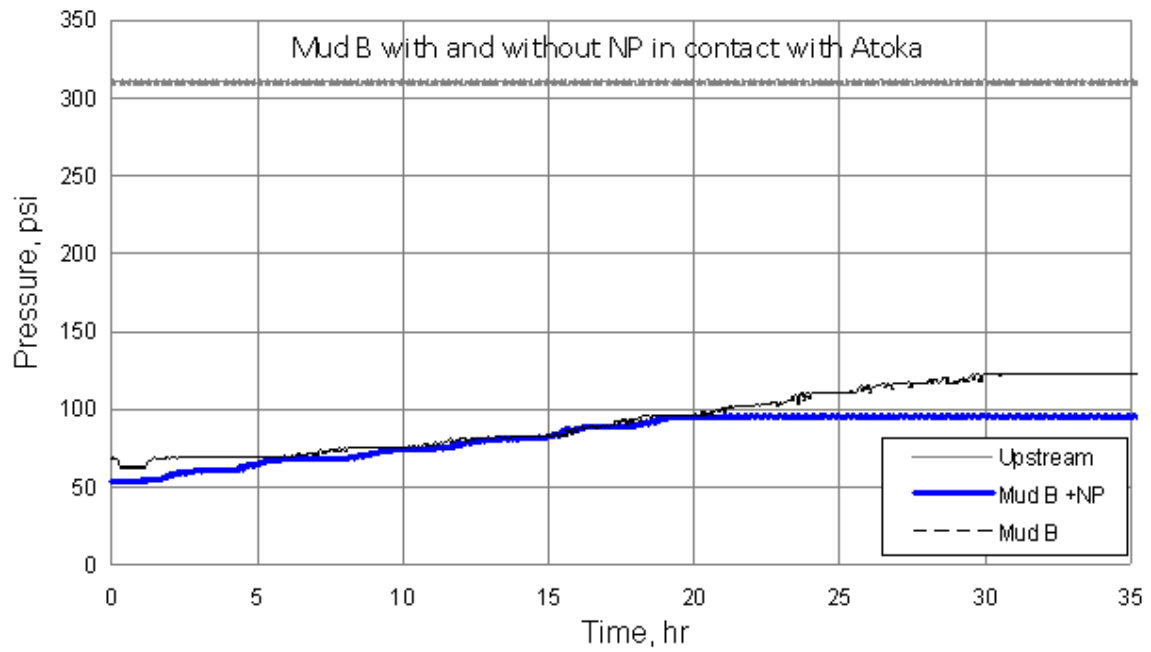


Figure 6.6: Comparison of Mud B with and without NP in contact with Atoka shale.

Table 6.5: Conditions for Test 6.4.

Test	6.4
Date	11/29/2008
Shale	Atoka
Brand	Nyacol 9711
Top Fluid	Mud B +NP
NP wt%	10
NP Size (nm)	20
Bottom Fluid	Brine
Aw top	0.93
Aw Bottom	0.98
Aw shale	0.98
Top Pres. (Psi)	340
Bottom Pres. (Psi)	50
Result	Stabilized at 240 psi differential pressure in 20 hours with a permeability of 0.0058 nd.

Table 6.6: Mud composition in Test 6.4.

Mud B+Nyacol NP	Volume, cc	Mass, gr
Mud solid	17.94	48.97
mud water	79.03	79.03
mud total	96.97	128.00
NP solid	10.13	16.80
NP sol. water	23.20	23.20
NP sol. total	33.33	40.00
Total Solid %	21.5%	39.1%
NP %	7.8%	10.0%

Test 6.5 was performed to observe the response of Mud C in contact with Atoka shale. Table 6.7 shows the test conditions. As seen in Figure 6.7, the bottom pressure stabilized at 70 psi differential pressure in 32 hours. Using the transient method discussed in Chapter 4 the permeability of the sample was determined to be 0.028 nd.

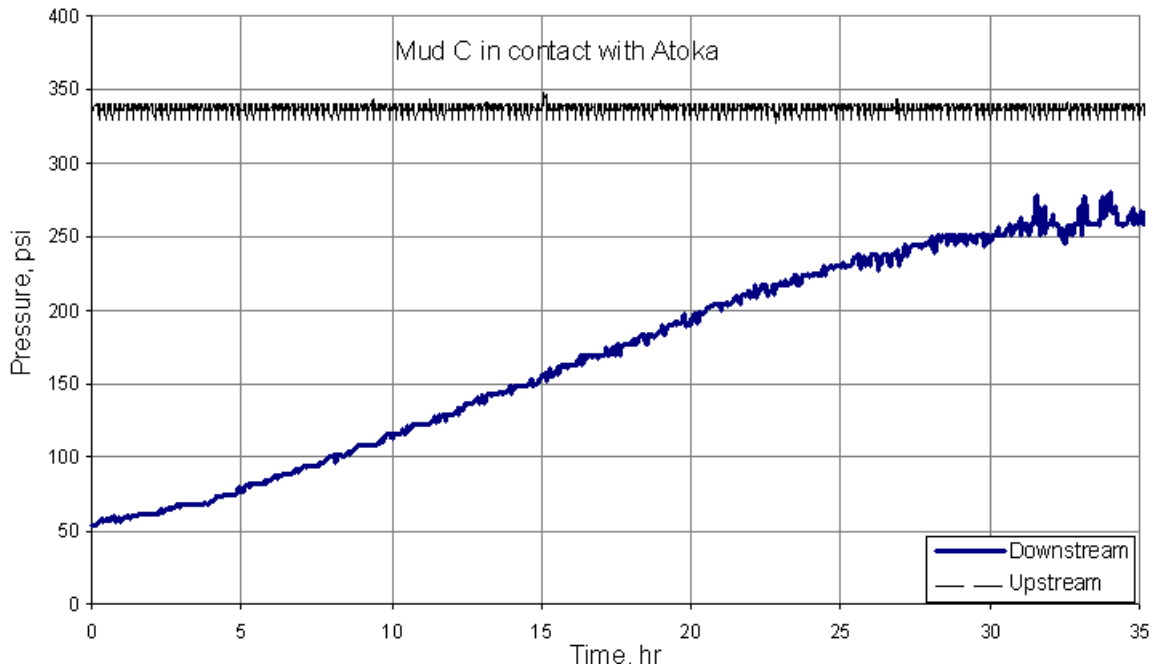


Figure 6.7: Results of Test 6.5 that was performed in contact with Atoka shale.

Table 6.7: Conditions for Test 6.5.

Test	6.5
Date	12/1/2008
Shale	Atoka
Top Fluid	Mud C
NP wt%	0
Bottom Fluid	Brine
Aw top	0.98
Aw Bottom	0.98
Aw shale	0.98
Top Pres. (Psi)	340
Bottom Pres. (Psi)	50
Result	Stabilized at 80 psi differential pressure in 30 hours with a permeability of 0.028 nd.

Test 6.6 was performed to observe the effect of NP's on the response of Mud C in contact with Atoka shale. Table 6.8 and Table 6.9 show the test conditions. As seen in Figure 6.8, the bottom pressure stabilized at 120 psi differential pressure in 40 hours. As shown in Figure 6.9, adding Nyacol's silica NP dispersion to the Field Mud C reduced the fluid penetration by 38 % in 36 hours. Using the transient method discussed in Chapter 4 the permeability of the sample was determined to be 0.0114 nd.

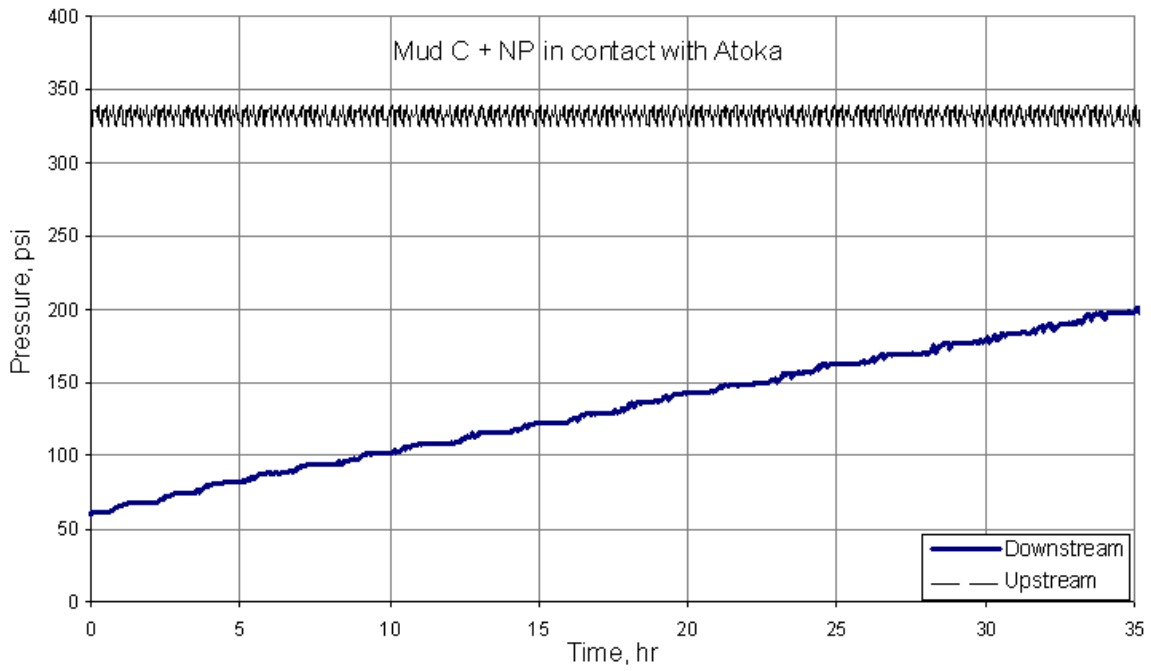


Figure 6.8: Results of Test 6.6 that was performed in contact with Atoka shale.

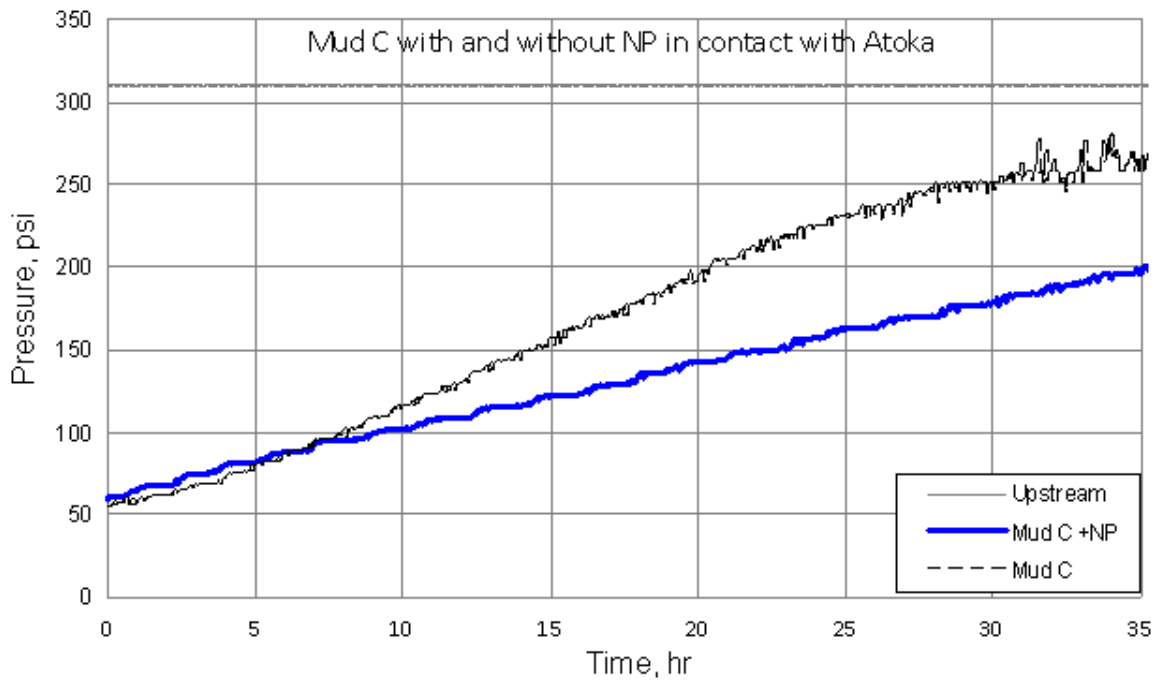


Figure 6.9: Comparison of Mud C with and without NP in contact with Atoka shale.

Table 6.8: Conditions for Test 6.6

Test	6.6
Date	12/15/2008
Shale	Atoka
Brand	Nyacol 9711
Top Fluid	Mud C+ NP
NP wt%	10
NP Size (nm)	20
Bottom Fluid	Brine
Aw top	0.98
Aw Bottom	0.98
Aw shale	0.98
Top Pres. (Psi)	335
Bottom Pres. (Psi)	55
Result	Stabilized at 120 psi differential pressure in 40 hours with a permeability of 0.0114 nd.

Table 6.9: Mud composition in Test 6.6

Mud C+Nyacol NP	Volume, cc	Mass, gr
Mud solid	21.14	34.86
mud water	93.14	93.14
mud total	114.29	128.00
NP solid	10.13	16.80
NP sol. water	23.20	23.20
NP sol. total	33.33	40.00
Total Solid %	21.2%	30.7%
NP %	6.9%	10.0%

Test 6.7 was performed to observe the response of Mud D in contact with Atoka shale. Table 6.10 shows the test conditions. As seen in Figure 6.10, the bottom pressure stabilized at 150 psi differential pressure in 40 hours. Using the transient method discussed in Chapter 4 the permeability of the sample was determined to be 0.0056 nd.

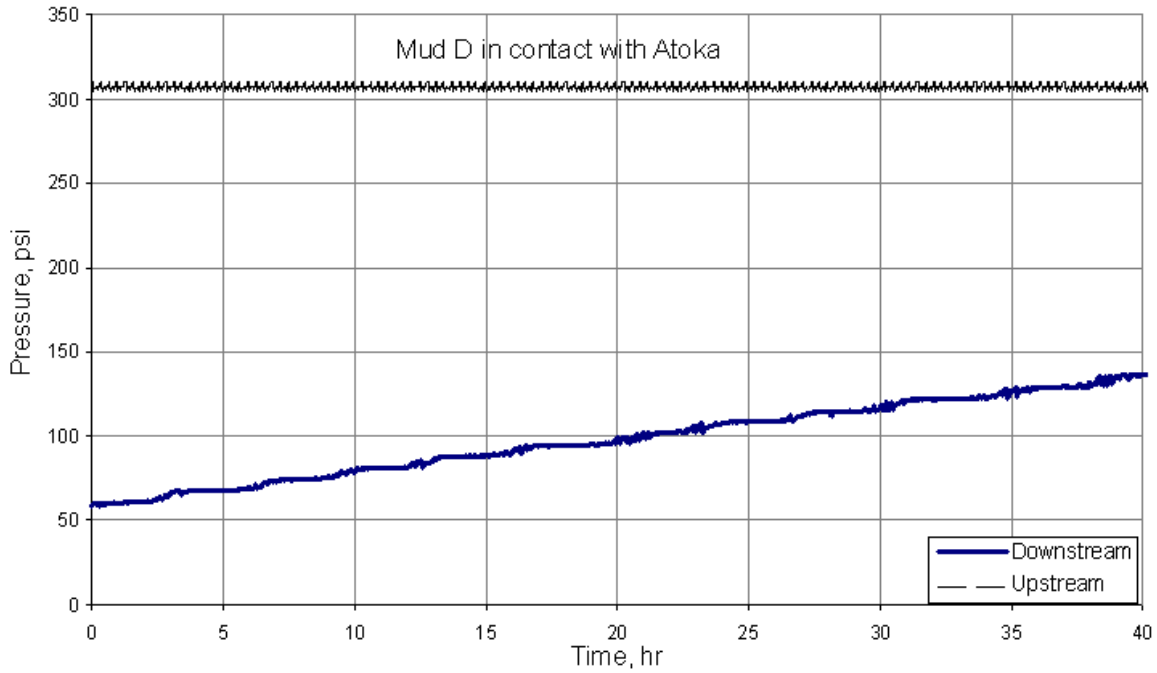


Figure 6.10: Results of Test 6.7 that was performed in contact with Atoka shale.

Table 6.10: Conditions for Test 6.7.

Test	6.7
Date	12/18/2008
Shale	Atoka
Top Fluid	Mud D
NP wt%	0
Bottom Fluid	Brine
Aw top	1
Aw Bottom	0.98
Aw shale	0.98
Top Pres. (Psi)	305
Bottom Pres. (Psi)	55
Result	Stabilized at 150 psi differential pressure in 40 hours with a permeability of 0.0056nd.

Test 6.8 was performed to observe the effect of NP's on the response of Mud D in contact with Atoka shale. Table 6.11 shows the test conditions and Table 6.12 shows the mud composition. As seen in Figure 6.11, the bottom pressure stabilized at 200 psi differential pressure in 30 hours. As shown in Figure 6.12, adding Nyacol's silica NP dispersion to the Field Mud D reduced the fluid penetration by 25 % in 36 hours. Using the transient method discussed in Chapter 4 the permeability of the sample was determined to be 0.004 nd.

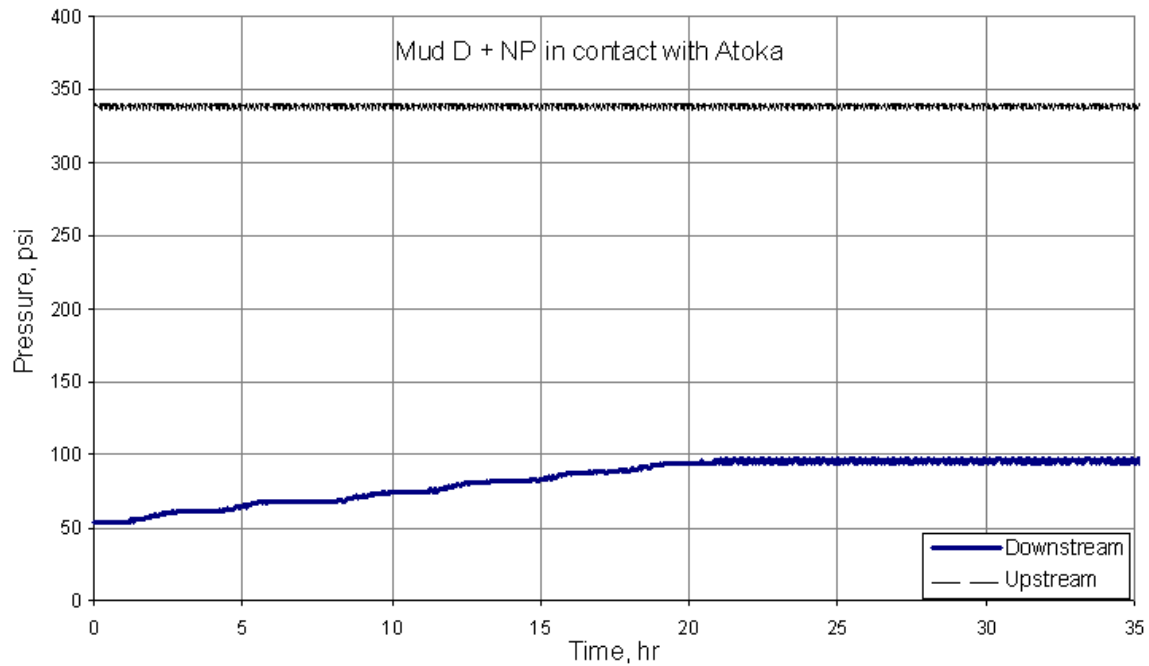


Figure 6.11: Results of Test 6.8 that was performed in contact with Atoka shale.

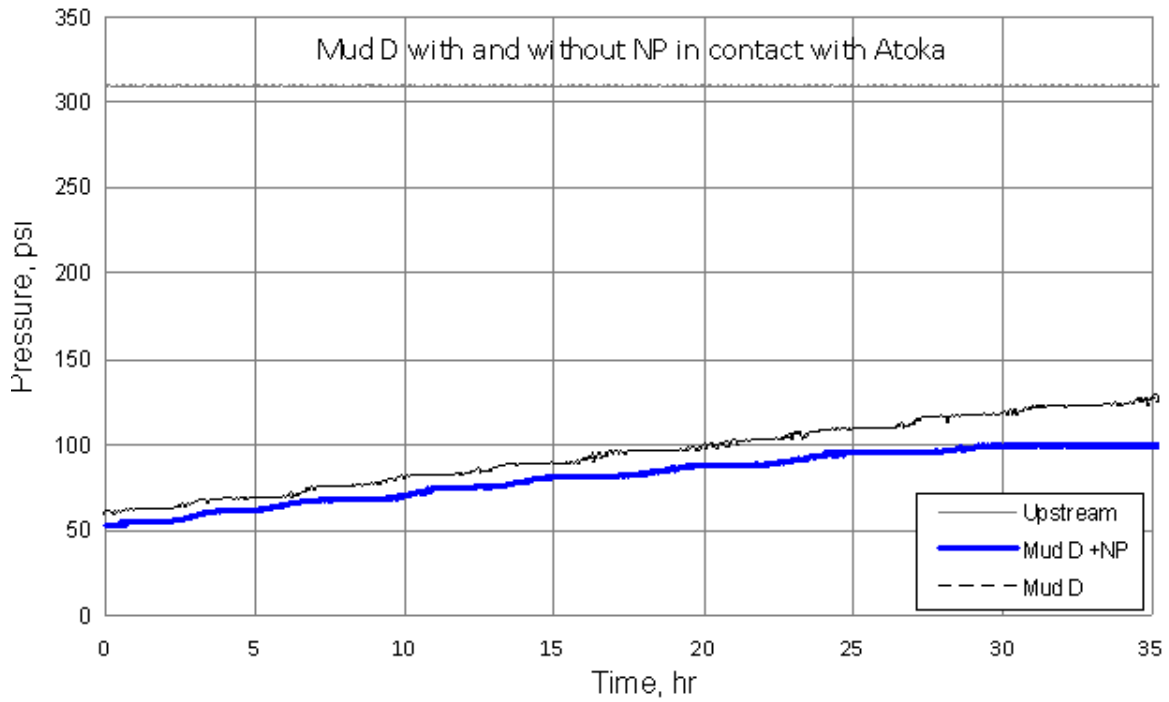


Figure 6.12: Comparison of Mud D with and without NP in contact with Atoka shale.

Table 6.11: Conditions for Test 6.8.

Test	6.8
Date	12/19/2008
Shale	Atoka
Brand	Nyacol 9711
Top Fluid	Mud D+ NP
NP wt%	10
NP Size (nm)	20
Bottom Fluid	Brine
Aw top	1
Aw Bottom	0.98
Aw shale	0.98
Top Pres. (Psi)	300
Bottom Pres. (Psi)	50
Result	Stabilized at 200 psi differential pressure in 30 hours with a permeability of 0.0056 nd.

Table 6.12: Mud composition in Test 6.8.

Mud D+Nyacol NP	Volume, cc	Mass, gr
Mud solid	12.03	30.63
mud water	97.37	97.37
mud total	109.40	128.00
NP solid	10.13	16.80
NP sol. water	23.20	23.20
NP sol. total	33.33	40.00
Total Solid %	15.5%	28.2%
NP %	7.1%	10.0%

Permeability calculations for each field mud test are done to observe the effect of nanoparticles. As seen in Figure 6.13 and Table 6.13, nanoparticle additions to field muds reduced the permeability of Atoka shale by factor of 11 for Field Mud A, 2.45 for Field Mud C and 1.4 for Field Mud D.

Table 6.13: Permeability values obtained with and without nanoparticles for Atoka

Test	Rock	Fluid	Permeability (nd)
4	Atoka	Brine	0.41
24	Atoka	Mud A	0.044
25	Atoka	Mud A Modified	0.0038
27	Atoka	Mud B	0.0047
28	Atoka	Mud B Modified	0.0058
29	Atoka	Mud C	0.028
32	Atoka	Mud C Modified	0.0114
33	Atoka	Mud D	0.0056
34	Atoka	Mud D Modified	0.004

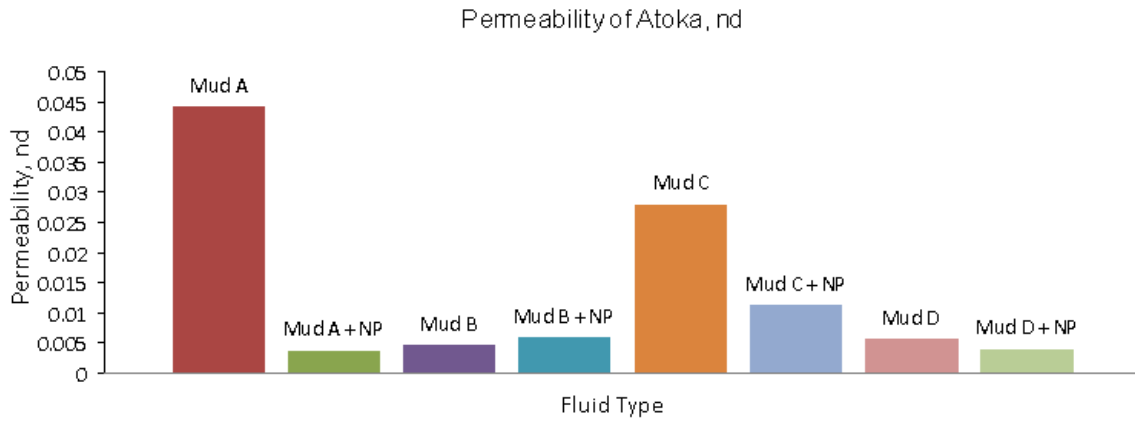


Figure 6.13: Permeability chart of Atoka shale

6.2 Field Muds in contact with GOM shale

Test 6.9 was performed to observe the response of Mud A in contact with GOM shale. Table 6.14 shows the test conditions. As seen in Figure 6.14, the bottom pressure stabilized at 70 psi differential pressure in 20 hours. Using the transient method discussed in Chapter 4 the permeability of the sample was determined to be 0.038 nd.

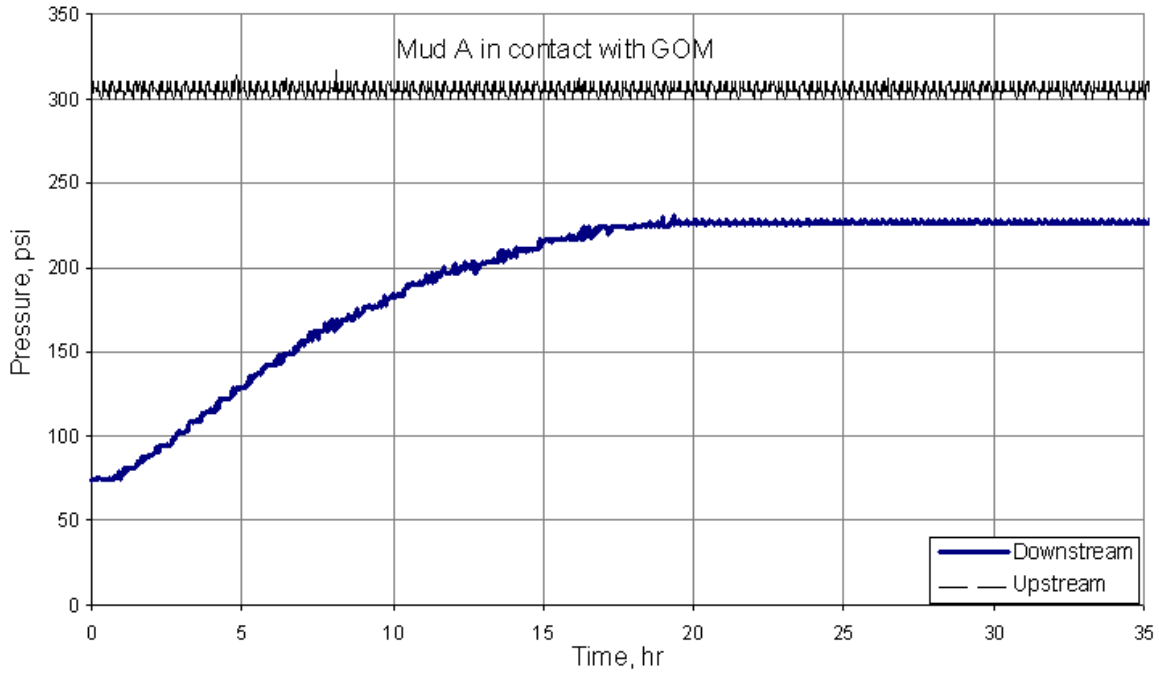


Figure 6.14: Results of Test 6.9 that was performed in contact with GOM shale.

Table 6.14: Conditions for Test 6.9.

Test	6.9
Date	12/12/2008
Shale	GOM
Top Fluid	Mud A
NP wt%	0
Bottom Fluid	Brine
Aw top	1
Aw Bottom	0.98
Aw shale	0.98
Top Pres. (Psi)	300
Bottom Pres. (Psi)	70
Result	Stabilized at 70 psi differential pressure in 20 hours with a permeability of 0.038 nd.

Test 6.10 was performed to observe the effect of NP's on the response of Field Mud A in contact with GOM shale. Table 6.15 shows the test conditions and Table 6.16 shows the mud composition. As seen in Figure 6.15, the bottom pressure stabilized at 70 psi differential pressure in 20 hours. As shown in Figure 6.16, adding Nyacol's silica NP dispersion to the Field Mud A reduced the fluid penetration by 27 % in 36 hours. Using the transient method discussed in Chapter 4 the permeability of the sample was determined to be 0.014 nd.

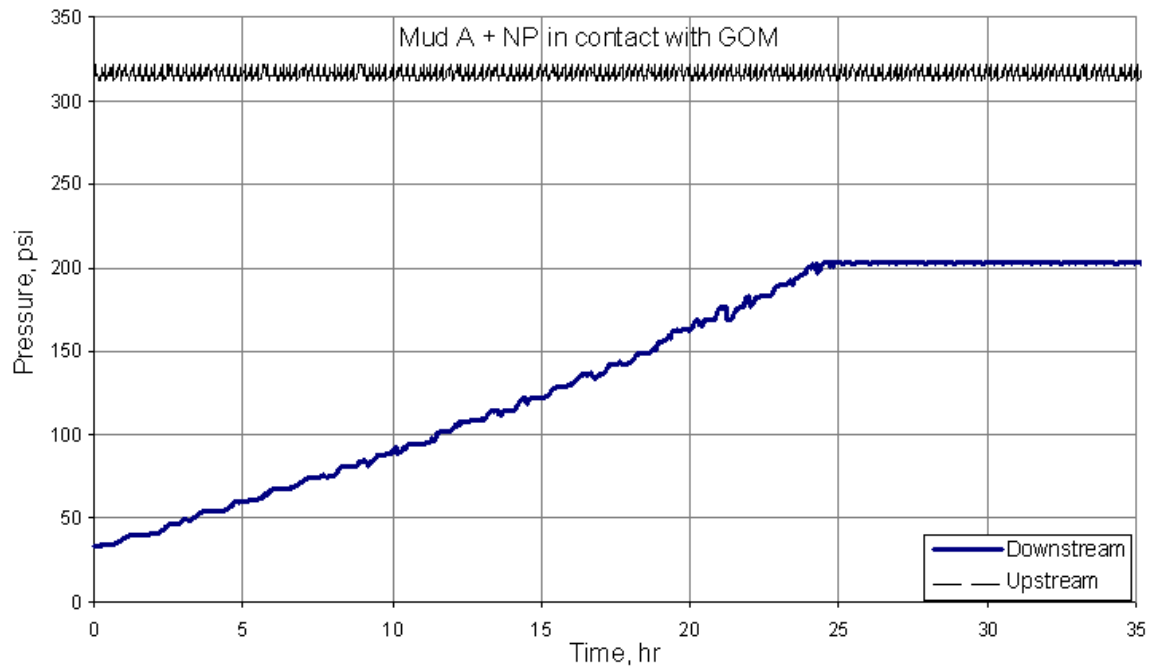


Figure 6.15: Results of Test 6.10 that was performed in contact with GOM shale.

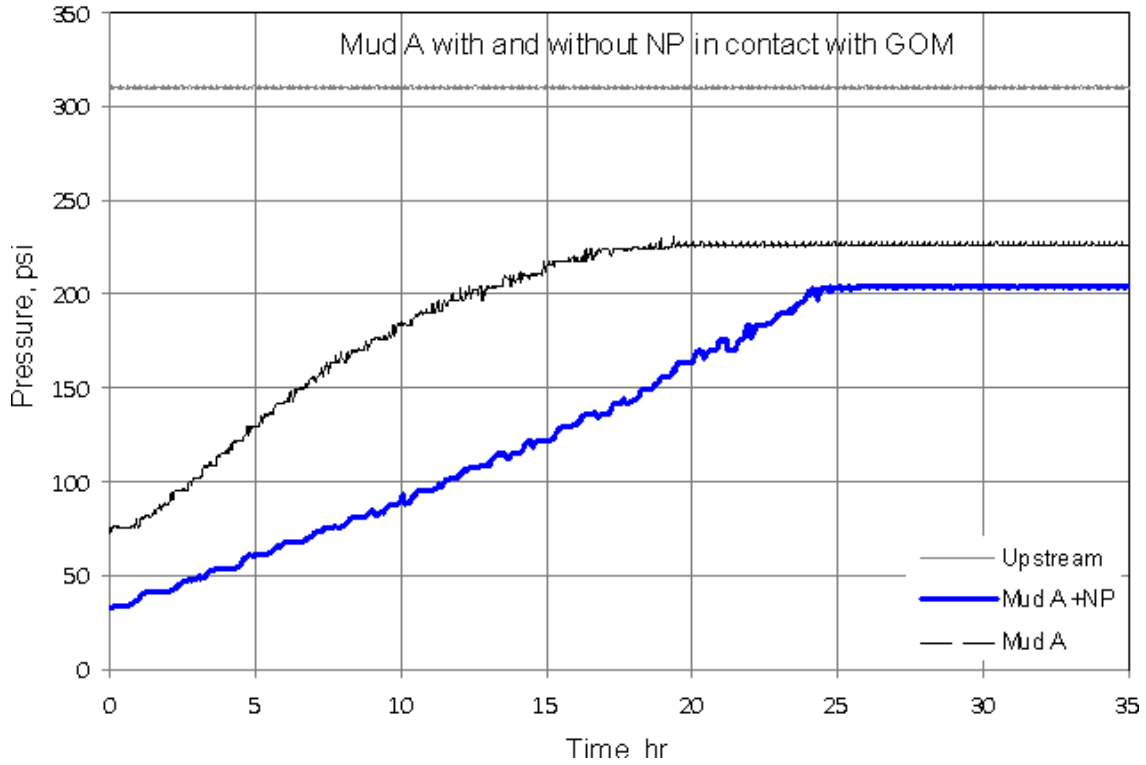


Figure 6.16: Comparison of Mud A with and without NP in contact with GOM shale.

Table 6.15: Conditions for Test 6.10.

Test	6.10
Date	12/14/2008
Shale	GOM
Brand	Nyacol 9711
Top Fluid	Mud A + NP
NP wt%	10
NP Size (nm)	20
Bottom Fluid	Brine
Aw top	1
Aw Bottom	0.98
Aw shale	0.98
Top Pres. (Psi)	315
Bottom Pres. (Psi)	40
Result	Stabilized at 140 psi differential pressure in 24 hours with a permeability of 0.014 D.

Table 6.16: Mud composition in Test 6.10

Mud A+Nyacol NP	Volume, cc	Mass, gr
Mud solid	17.33	56.44
mud water	71.56	71.56
mud total	88.89	128.00
NP solid	10.13	16.80
NP sol. water	23.20	23.20
NP sol. total	33.33	40.00
Total Solid %	22.5%	43.6%
NP %	8.3%	10.0%

Test 6.11 was performed to observe the response of Mud B in contact with GOM shale. Table 6.17 shows the test conditions. As seen in Figure 6.17, the bottom pressure stabilized at 120 psi differential pressure in 11 hours. Using the transient method discussed in Chapter 4 the permeability of the sample was determined to be 0.0404 nd.

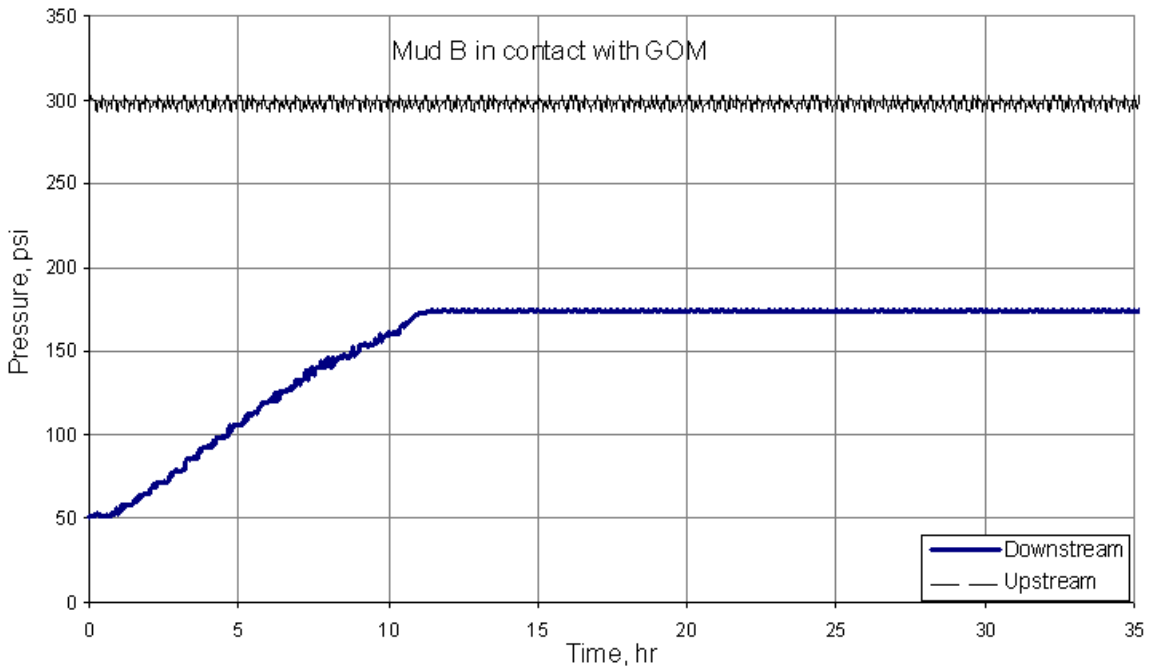


Figure 6.17: Results of Test 6.11 that was performed in contact with GOM shale.

Table 6.17: Conditions for Test 6.11.

Test	6.11
Date	12/20/2008
Shale	GOM
Top Fluid	Mud B
NP wt%	0
Bottom Fluid	Brine
Aw top	0.93
Aw Bottom	0.98
Aw shale	0.98
Top Pres. (Psi)	300
Bottom Pres. (Psi)	50
Result	Stabilized at 120 psi differential pressure in 11 hours with a permeability of 0.0404 nd.

Test 6.12 was performed to observe the effect of NP's on the response of Mud B in contact with GOM shale. Table 6.18 shows the test conditions and Table 6.19 shows the mud composition. As seen in Figure 6.18, the bottom pressure stabilized at 150 psi differential pressure in 10 hours. As shown in Figure 6.19, adding Nyacol's silica NP dispersion to the Field Mud B reduced the fluid penetration by 25 % in 36 hours. Using the transient method discussed in Chapter 4 the permeability of the sample was determined to be 0.0408 nd.

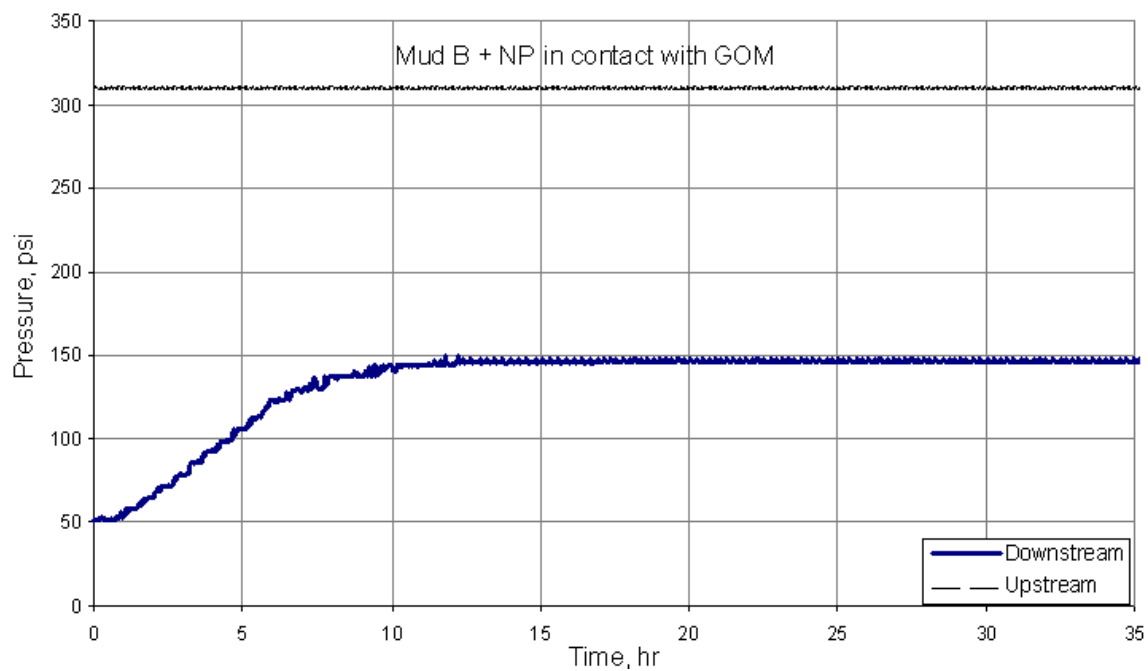


Figure 6.18: Results of Test 6.12 that was performed in contact with GOM shale.

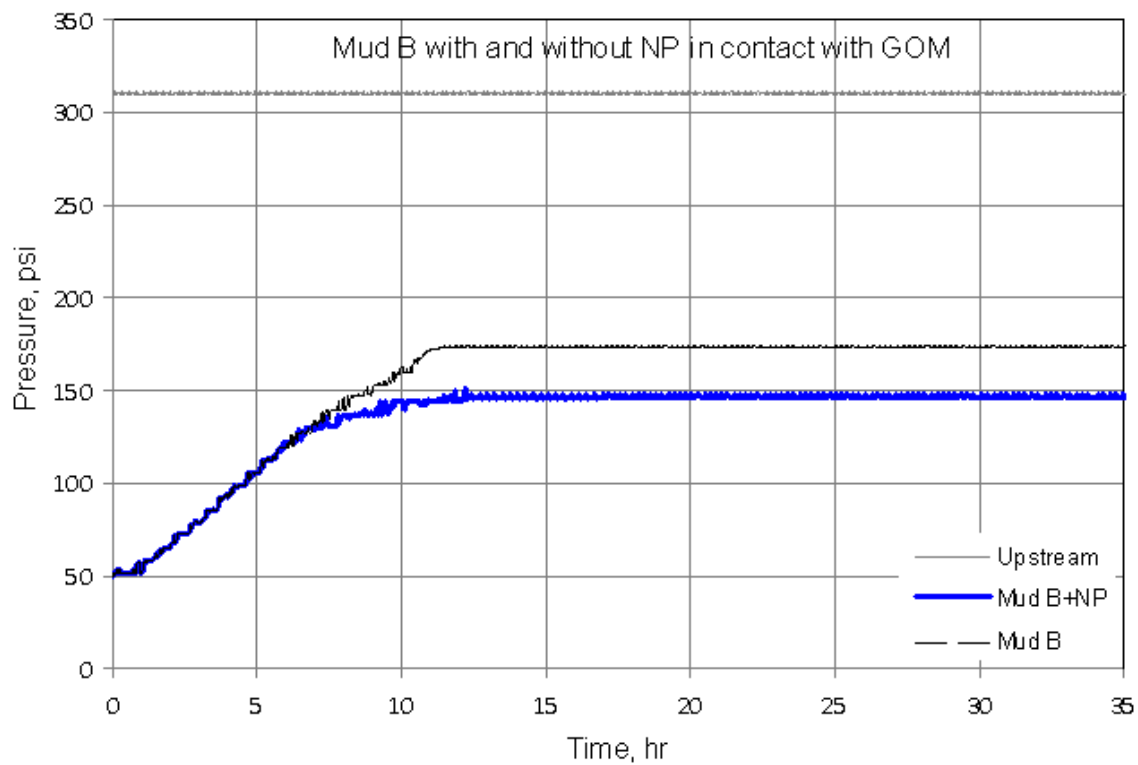


Figure 6.19: Comparison of Mud B with and without NP in contact with GOM shale.

Table 6.18: Conditions for Test 6.12.

Test	6.12
Date	12/22/2008
Shale	GOM
Brand	Nyacol 9711
Top Fluid	Mud B+ NP
NP wt%	10
NP Size (nm)	20
Bottom Fluid	Brine
Aw top	0.93
Aw Bottom	0.98
Aw shale	0.98
Top Pres. (Psi)	310
Bottom Pres. (Psi)	50
Result	Stabilized at 160 psi differential pressure in 10 hours with a permeability of 0.0408 nd.

Table 6.19: Mud composition in Test 6.12.

Mud B+Nyacol NP	Volume, cc	Weight, gr
Mud solid	17.94	48.97
mud water	79.03	79.03
mud total	96.97	128.00
NP solid	10.13	16.80
NP sol. water	23.20	23.20
NP sol. total	33.33	40.00
Total Solid %	21.5%	39.1%
NP %	7.8%	10.0%

Test 6.13 was performed to observe the response of Mud C in contact with GOM shale. Table 6.20 shows the test conditions. As seen in Figure 6.20, the bottom pressure stabilized at 100 psi differential pressure in 27 hours. Using the transient method discussed in Chapter 4 the permeability of the sample was determined to be 0.0203 nd.

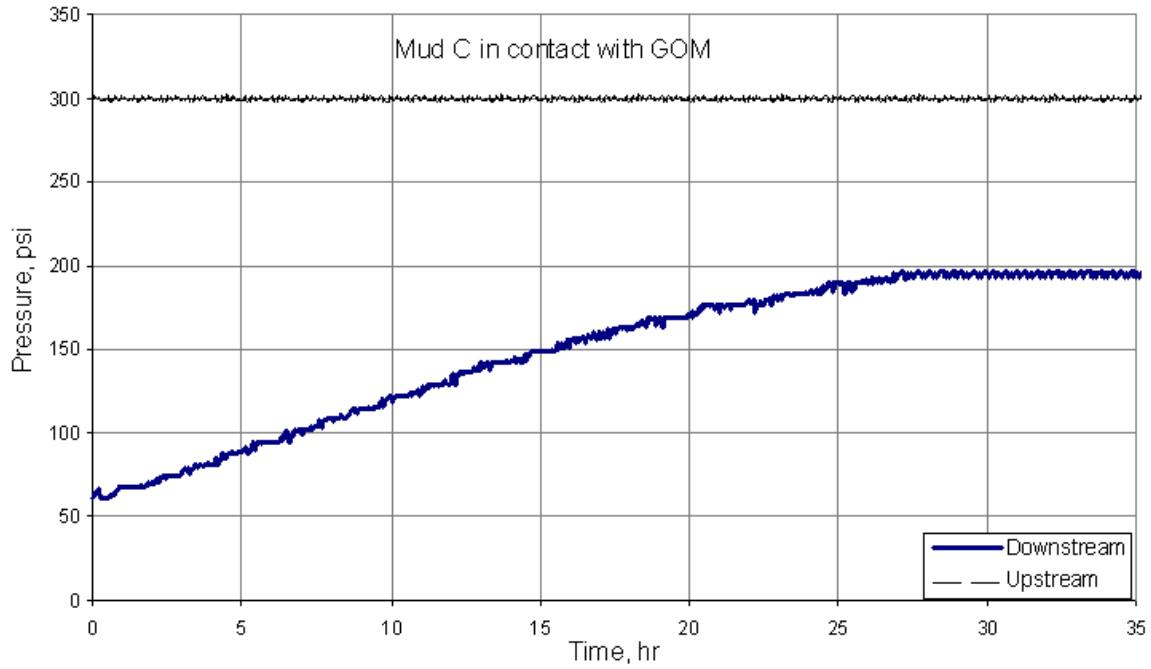


Figure 6.20: Results of Test 6.13 that was performed in contact with GOM shale.

Table 6.20: Conditions for Test 6.13.

Test	6.13
Date	12/25/2008
Shale	GOM
Top Fluid	Mud C
NP wt%	0
Bottom Fluid	Brine
Aw top	0.98
Aw Bottom	0.98
Aw shale	0.98
Top Pres. (Psi)	300
Bottom Pres. (Psi)	50
Result	Stabilized at 100 psi differential pressure in 27 hours with a permeability of 0.0203 nd.

Test 6.14 was performed to observe the effect of NP's on the response of Mud C in contact with GOM shale. Table 6.21 shows the test conditions and Table 6.22 shows the mud composition. As seen in Figure 6.21, the bottom pressure stabilized at 120 psi differential pressure in 35 hours. As shown in Figure 6.22, adding Nyacol's silica NP dispersion to the Field Mud C reduced the fluid penetration by 20 % in 36 hours. Using the transient method discussed in Chapter 4 the permeability of the sample was determined to be 0.0126 nd.

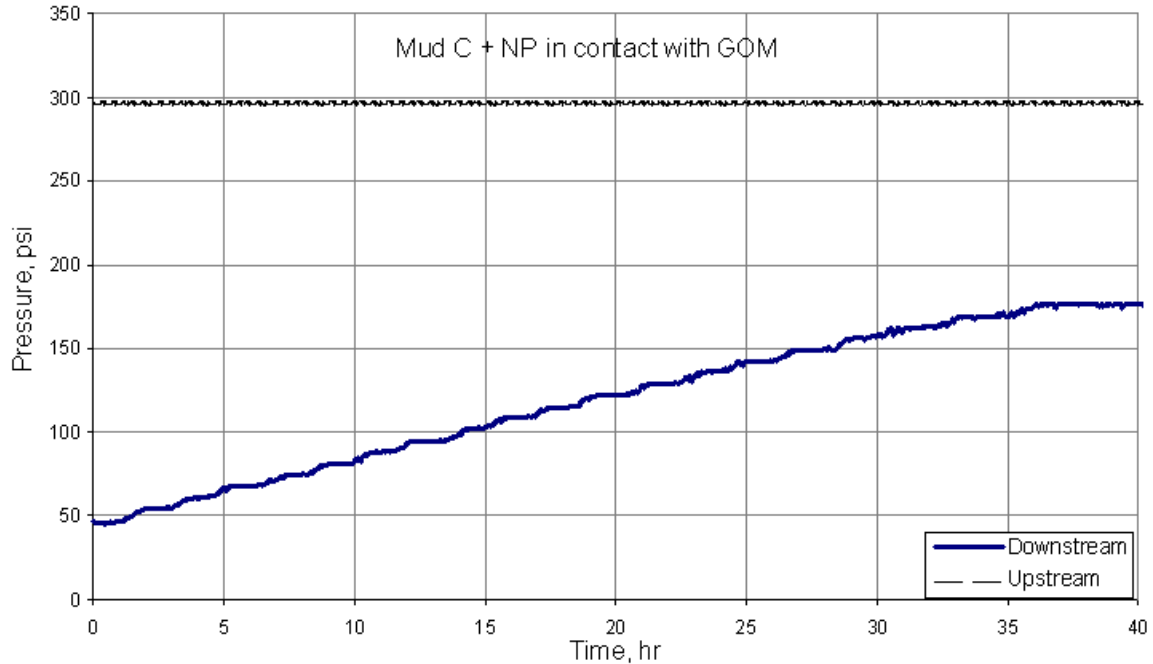


Figure 6.21: Results of Test 6.14 that was performed in contact with GOM shale.

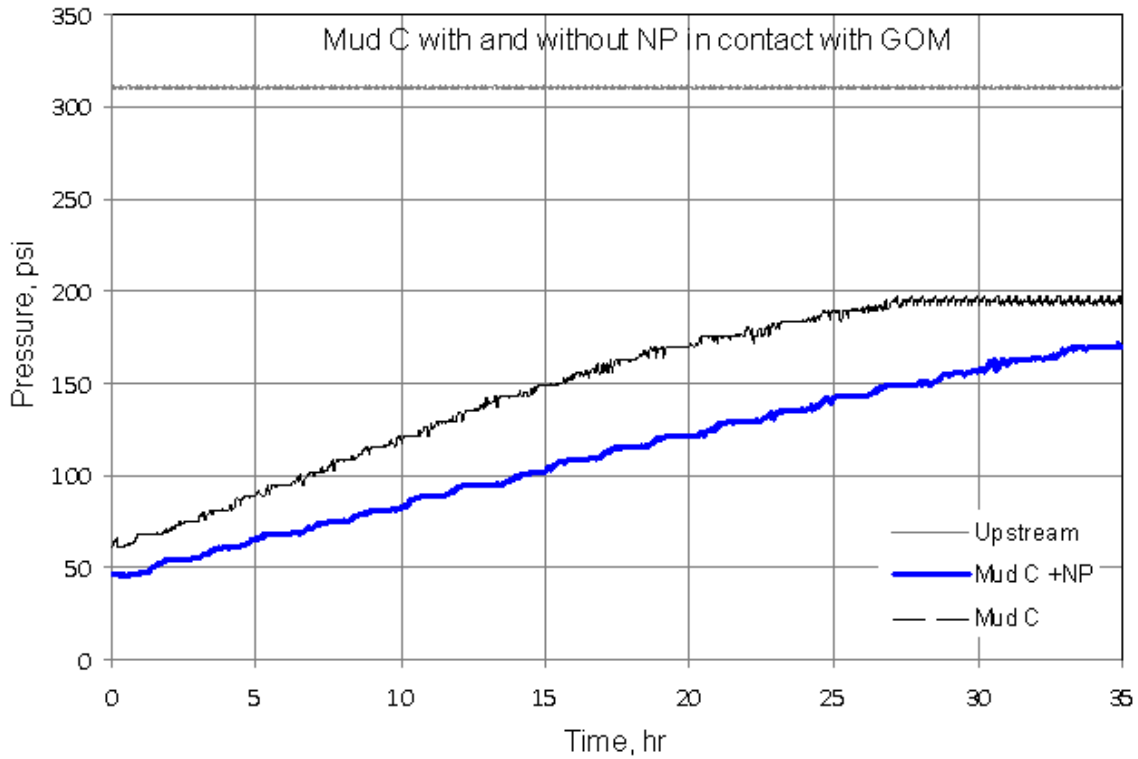


Figure 6.22: Comparison of Mud C with and without NP in contact with GOM shale.

Table 6.21: Conditions for Test 6.14.

Test	6.14
Date	12/25/2008
Shale	GOM
Brand	Nyacol 9711
Top Fluid	Mud C + NP
NP wt%	10
NP Size (nm)	20
Bottom Fluid	Brine
Aw top	0.98
Aw Bottom	0.98
Aw shale	0.98
Top Pres. (Psi)	295
Bottom Pres. (Psi)	50
Result	Stabilized at 120 psi differential pressure in 36 hours with a permeability of 0.0126 nd.

Table 6.22: Mud composition in Test 6.14

Mud C+Nyacol NP	Volume, cc	Mass, gr
Mud solid	21.14	34.86
mud water	93.14	93.14
mud total	114.29	128.00
NP solid	10.13	16.80
NP sol. water	23.20	23.20
NP sol. total	33.33	40.00
Total Solid %	21.2%	30.7%
NP %	6.9%	10.0%

Test 6.15 was performed to observe the response of Mud D in contact with GOM shale. Table 6.23 shows the test conditions. As seen in Figure 6.23, bottom pressure kept the differential pressure at 150 psi for 35 hours. Using the transient method discussed in Chapter 4 the permeability of the sample was determined to be 0.0109 nd.

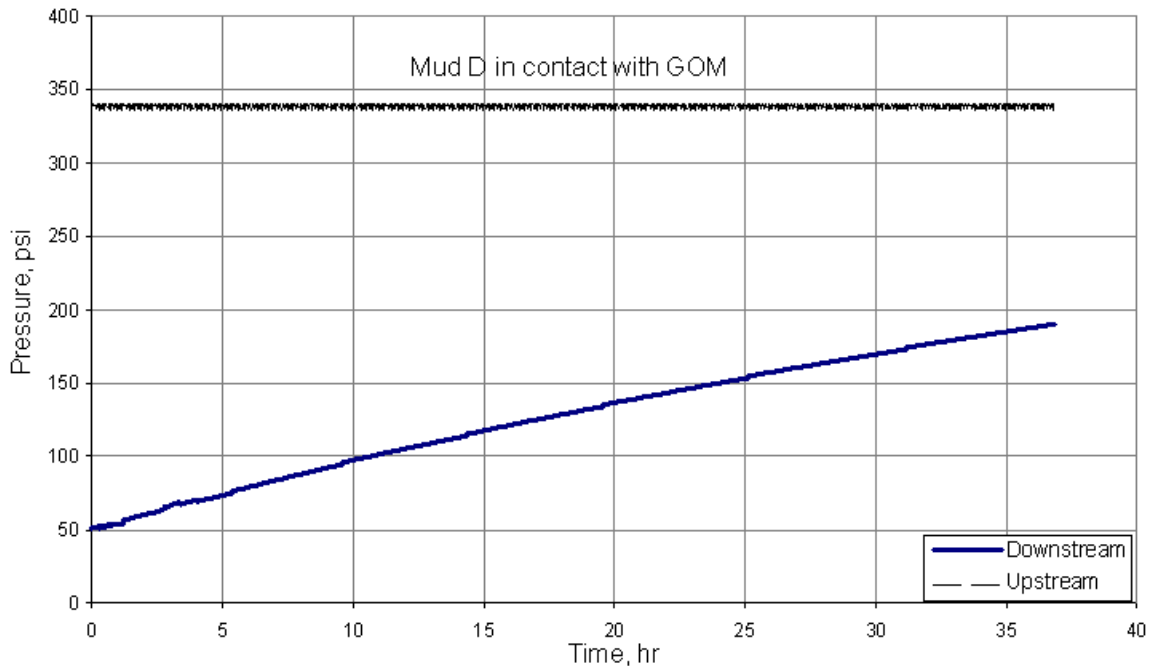


Figure 6.23: Results of Test 6.15 that was performed in contact with GOM shale.

Table 6.23: Conditions for Test 6.15.

Test	6.15
Date	12/27/2008
Shale	GOM
Top Fluid	Mud D
NP wt%	0
Bottom Fluid	Brine
Aw top	1
Aw Bottom	0.98
Aw shale	0.98
Top Pres. (Psi)	340
Bottom Pres. (Psi)	50
Result	Kept the differential pressure at 140 psi for 36 hours with a permeability of 0.0109 nd.

Test 6.16 was performed to observe the effect of NP's on the response of Mud D in contact with GOM shale. Table 6.24 shows the test conditions and Table 6.25 shows the mud composition used for the test. As seen in Figure 6.24, the bottom pressure stabilized at 170 psi differential pressure in 36 hours. As shown in Figure 6.25, adding Nyacol's silica NP dispersion to the Field Mud D reduced the fluid penetration by 17 % in 36 hours. Using the transient method discussed in Chapter 4 the permeability of the sample was determined to be 0.007 nd.

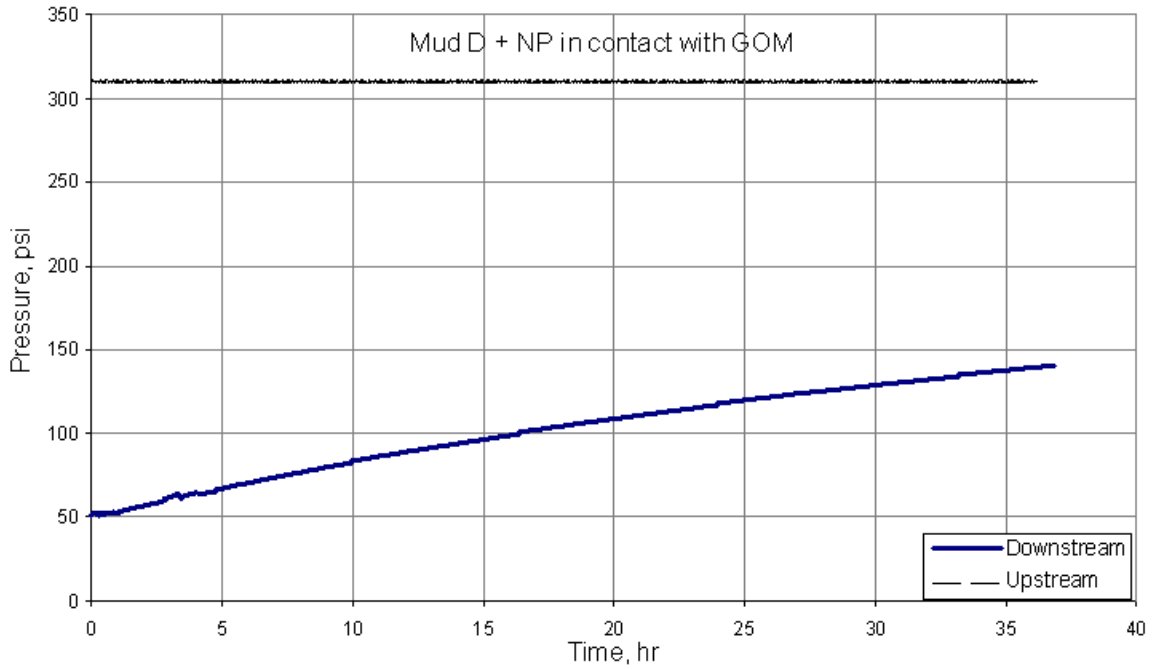


Figure 6.24: Results of Test 6.16 that was performed in contact with GOM shale.

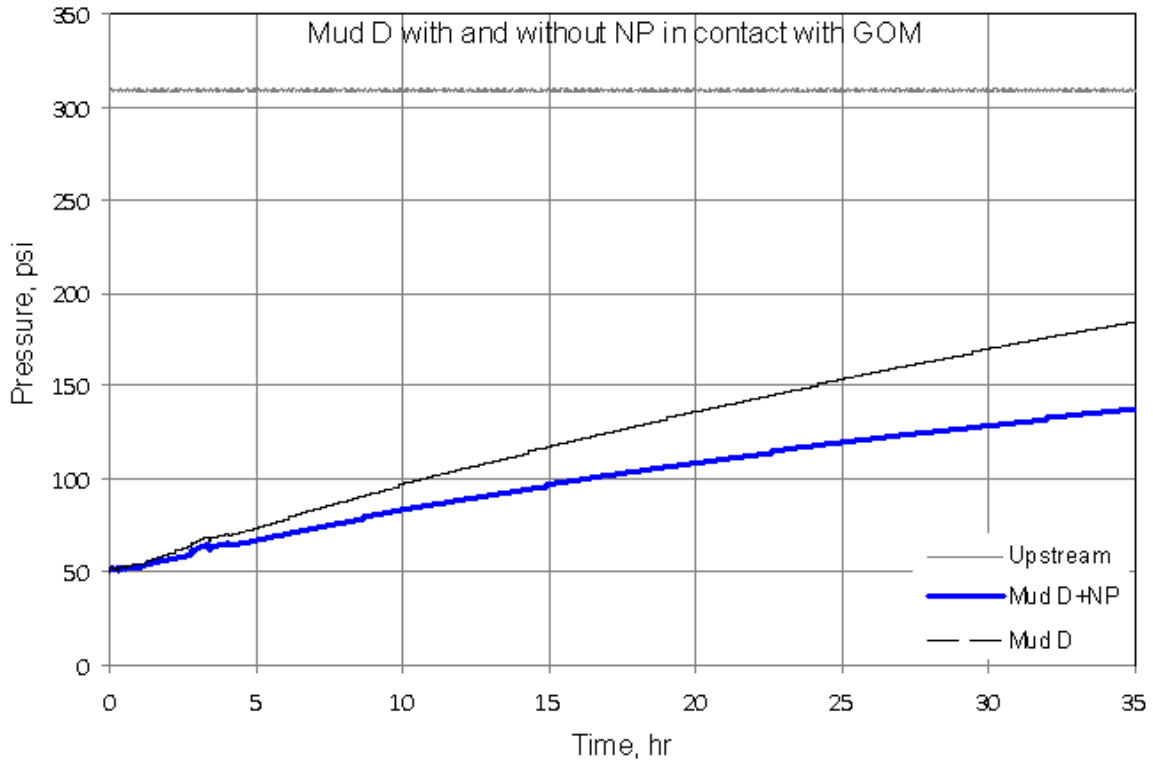


Figure 6.25: Comparison of Mud D with and without NP in contact with GOM shale.

Table 6.24: Conditions for Test 6.16.

Test	6.16
Date	12/29/2008
Shale	GOM
Brand	Nyacol 9711
Top Fluid	Mud D + NP
NP wt%	10
NP Size (nm)	20
Bottom Fluid	Brine
Aw top	1
Aw Bottom	0.98
Aw shale	0.98
Top Pres. (Psi)	310
Bottom Pres. (Psi)	50
Result	Stabilized at 170 psi differential pressure in 36 hours with a permeability of 0.0070 nd.

Table 6.25: Composition in Test 6.16.

Mud D+Nyacol NP	Volume, cc	Mass, gr
Mud solid	12.03	30.63
mud water	97.37	97.37
mud total	109.40	128.00
NP solid	10.13	16.80
NP sol. water	23.20	23.20
NP sol. total	33.33	40.00
Total Solid %	15.5%	28.2%
NP %	7.1%	10.0%

Test 6.17 was performed to observe the response brine in contact with GOM shale. Table 6.26 shows the test conditions. As seen in Figure 6.26, the bottom pressure built up to the top pressure in 5 hours. Using the transient method discussed in Chapter 4 the permeability of the sample was determined to be 0.6510 nd.

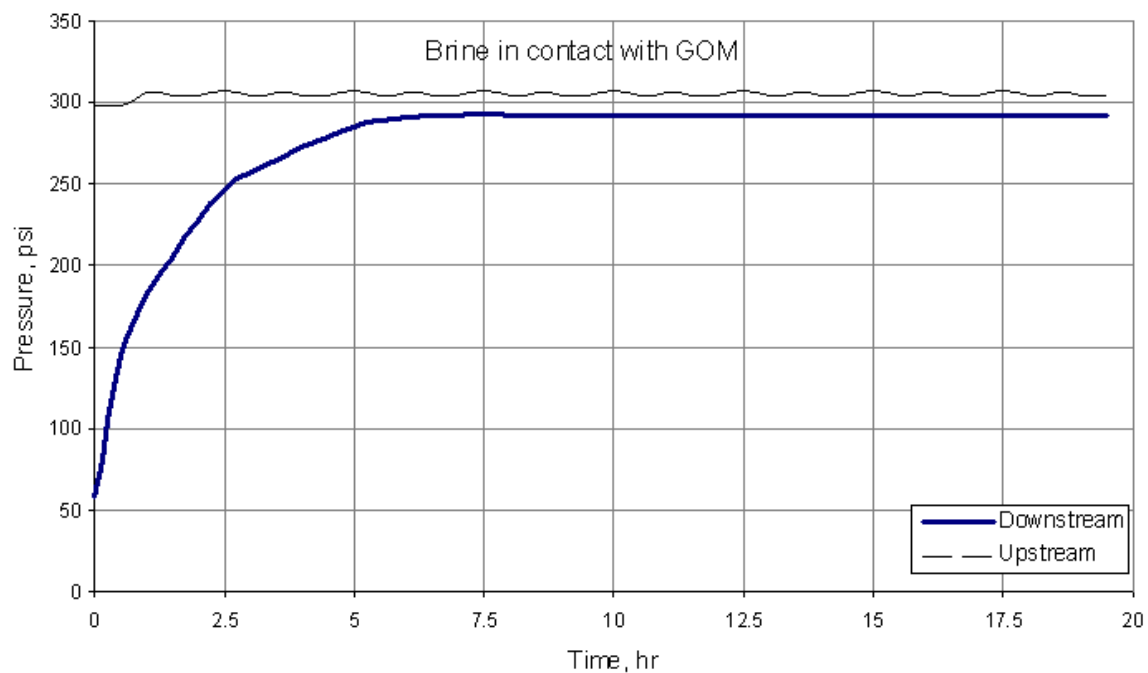


Figure 6.26: Results of Test 6.17 that was performed in contact with GOM shale.

Table 6.26: Conditions for Test 6.17

Test	6.17
Date	02/20/2009
Shale	GOM
Top Fluid	Brine
NP wt%	0
Bottom Fluid	Brine
Aw top	0.98
Aw Bottom	0.98
Aw shale	0.98
Top Pres. (Psi)	300
Bottom Pres. (Psi)	50
Result	Built up to the top pressure in 5 hours with a permeability of 0.6510 nd.

Permeability calculations for each field mud test were done to observe the effect of nanoparticles. As seen in Figure 6.27 and Table 6.27, Nanoparticle additions to the field muds reduced the permeability of GOM shale by factor of 2.76 for Field Mud A, 1.61 for Field Mud C and 1.55 for Field Mud D.

Table 6.27: Permeability values obtained with and without nanoparticles for GOM shale

Test	Rock	Fluid	Permeability (nd)
41	GOM	Brine	0.6510
30	GOM	Mud A	0.0380
31	GOM	Mud A Modified	0.0140
35	GOM	Mud B	0.0404
36	GOM	Mud B Modified	0.0408
37	GOM	Mud C	0.0203
38	GOM	Mud C Modified	0.0126
39	GOM	Mud D	0.0109
40	GOM	Mud D Modified	0.0070

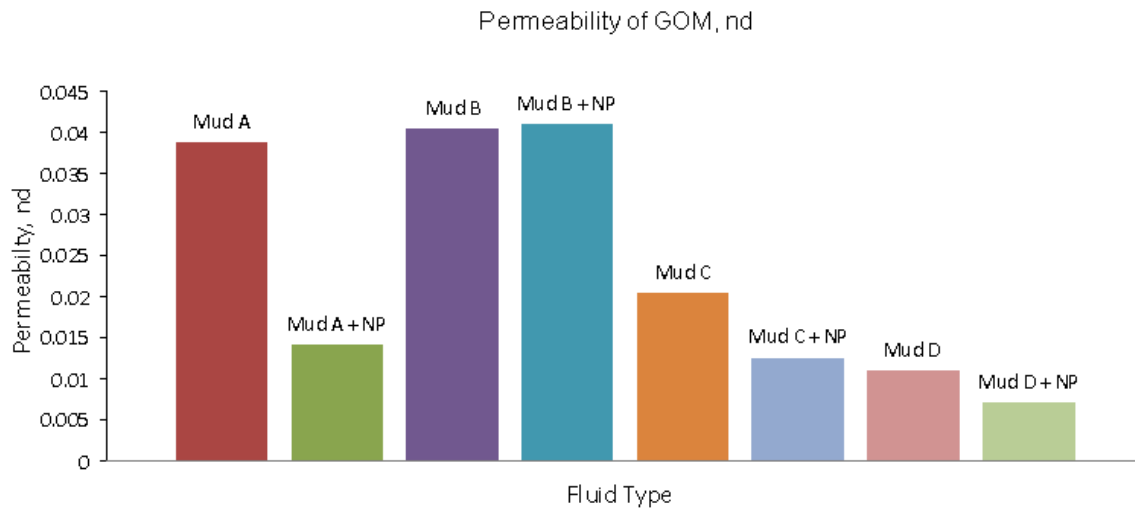


Figure 6.27: Permeability chart of GOM shale

Chapter 7

Conclusions and Future Work

In this study, it was shown that:

1. The use of nanoparticles reduced the fluid penetration into the Atoka shale up to 98 % compared to sea water.
2. The addition of nanoparticles to field muds reduced the fluid penetration into the Atoka shale by 16 to 72 %.
3. The addition of nanoparticle to field muds reduced the fluid penetration into the GOM shale by 17 to 27 %.
4. A water - nanoparticle dispersion can reduce the permeability of Atoka shale to less than 0.001 nd.
5. The minimum nanoparticle concentration needed to satisfactorily reduce the permeability and fluid invasion is 10 wt %, it was much better than 5 wt%.
6. By increasing the salt concentration of the mud the effectiveness of nanoparticle additions to the mud is reduced.
7. The best shale sealing performance for the Atoka shale is obtained with 20 nm size compared to 5 nm nanoparticles.
8. Some nanoparticle dispersions are not stable for condition of high salt concentration and temperature conditions.

Future Work:

1. A study of the effect of salt and nanoparticle concentrations is needed.
2. Different nanoparticle sizes should be obtained and mixtures of different sizes should be tried on each shale type to define the best mud-nanoparticle composition for every shale type.
3. Nano-clays may allow us to increase the nanoparticle concentration that can be used.

Appendix A

Shale Sample Preparation

Shale cores were covered and sealed with polyethylene at the rig-site before shipping. Shale cores were cut in our laboratory into 1.3" x 1.3" x 6" columns by using a 6" circular saw as shown in Figure A1. They were kept in Escaid oil in our laboratories to avoid any interaction between shale and air.



Figure A1: Circular 6" saw

Each column was glued to plastic bases using quick set epoxy, then covered with a 2.5" ID acrylic tube and allowed to dry for 5 minutes. The acrylic tube was also glued

to the base. (Figure A2) The key issue at this stage of preparation is to center the shale column carefully so it does not touch the acrylic tube.



Figure A2: Plastic tube placed on a base covering the shale column.

Using a 50/100 mixture by volume of Epicure and Epoxy Resin (purchased from Miller-Stephenson Company), was poured into the tube. On top of the shale was placed “a filler rock column”. This was done to facilitate handling. As shown in Figure A3, the epoxy mixture should rise above the filler rock column to make sure that the shale column is perfectly sealed.



Figure A3: The plastic tube containing shale and filler rock, filled with epoxy.

Epoxy set time is 6 to 7 days. Each tube is then sliced into 0.26" thick samples by using a 12" circular saw as shown in Figure A4. After slicing each disk, the outer plastic rings are removed and the disks are placed in one gallon cans that had been filled with Escaid oil. The final appearance of a shale disk is shown in Figure A5.



Figure A4: Circular 12” saw

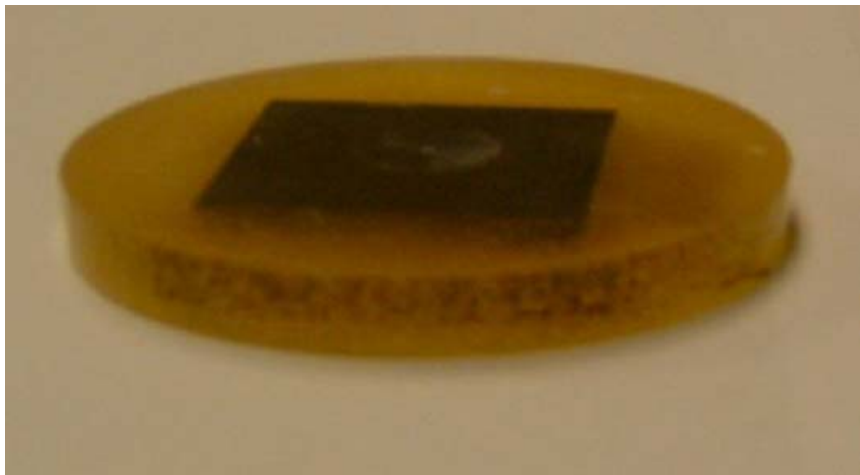


Figure A5: Final appearance of the shale disc ready to be placed in a desiccator

Each disk should be washed off with hexane and placed in a desiccator, Figure A6, which contains the desired humidity. Weight changes were observed over 2-3 days until the change merges to ± 0.001 grams. After the weight stabilization, the shale disks are ready for the fluid penetration tests.



Figure A6: Desiccators

Test Device

The test device is composed of a test cell, manual and syringe pumps, pressure transducers, exit pressure regulator, and the data accumulation system. The whole system is shown in Figure A7. A “zero volume” transducer, P9, supplied by Validyne Engineering type S/N/120388 is used to measure the pressure change of the 1.00 ml volume of sea water trapped below the test sample when valve V2 is closed.

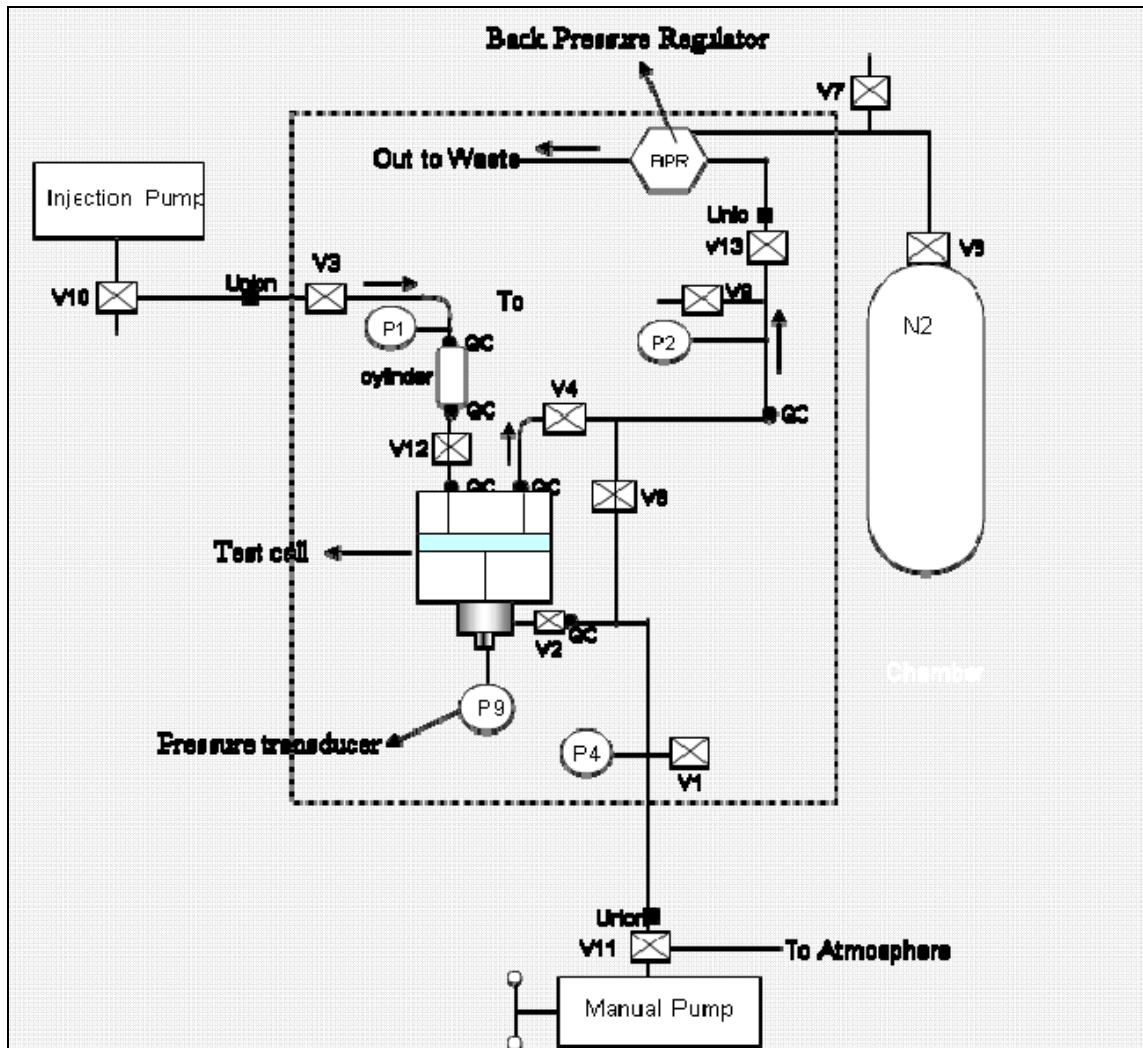


Figure A7: Configuration of the test device

The test cell is the component which holds the shale disk between two steel caps sealed with 2.5" x 0.228" O-rings. As seen in Figure A8, the O-rings are in contact with the epoxy sides of the disk and thereby seal the shale surface area. The top cap has two holes, one allows the top circulation fluid in and one allows the fluid out. The bottom cap has one hole which allows the application of bottom pressure to the shale. Three coarse

(18 mesh) layers of screen are placed on the top of the shale so as to apply a uniform pressure to the shale and also allow continuous flow over the surface. A coarse and a fine (18 and 117 mesh) screen layers are placed on the bottom of the shale disk for this same purpose.

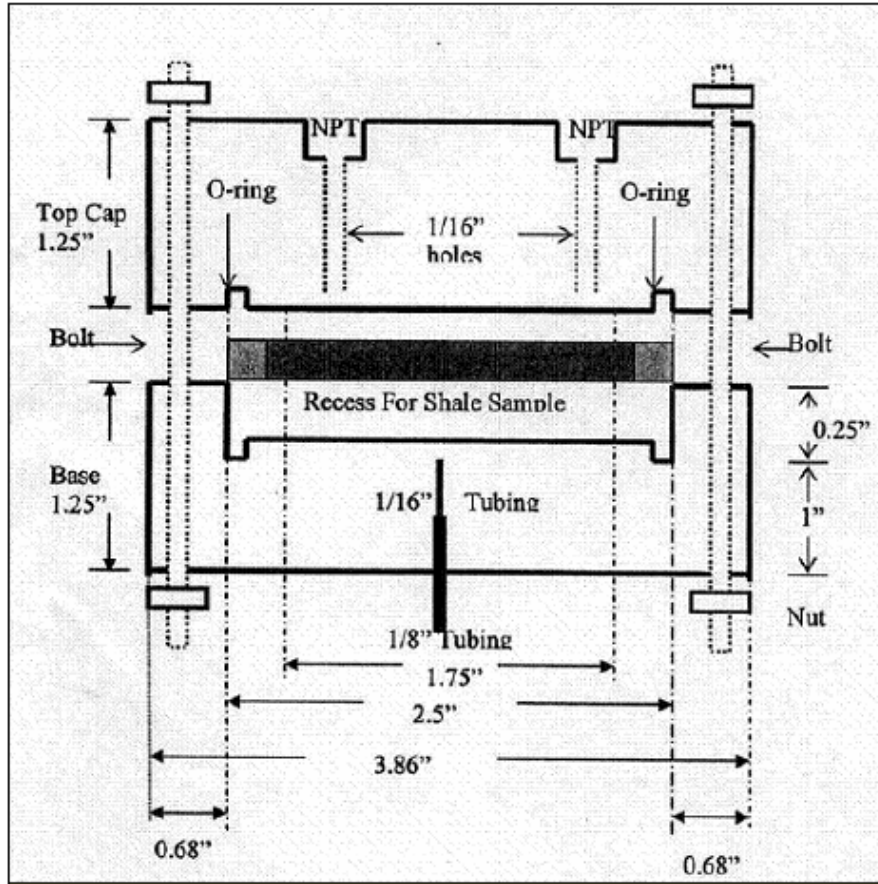


Figure A8: Test cell



Figure A9: Manual pump

After evacuating the air from the bottom chamber, the bottom fluid, a 0.98 Aw brine, was flowed into the chamber using a manual pump, Figure A9, so as to obtain the desired initiation bottom pressure. Valve 2 is then closed.

The top fluid was stored in a 160 ml capacity cylinder that contained a floating piston. The piston within the cylinder pushes the test mud out as water is injected into the opposite side of the piston using the syringe injection pump. The flow rate of the upstream fluid is controlled by the syringe pump as shown in Figure A10. The upstream

pressure is maintained at a constant pressure using a Mity Mite regulator that is connected to the Nitrogen cylinder shown in Figure A11.



Figure A10: Syringe pump

The data accumulation system was composed of 4 pressure transducers, a computer and a Texas Instruments Lab View device. Two pressure transducers are used to observe the pressures at the exit of the inlet mud chamber and two on the exit of the test cell. The bottom pressure is observed with a special zero volume transducer supplied by Validyne Engineering type S/N/120388 which allows detailed pressure observations. The data accumulation system is shown in Figure A11.



Figure A11: Data Accumulation system

References

1. Osuji, C., et al., Effect of Porosity and Permeability on the Membrane Efficiency of Shales, The University of Texas at Austin, SPE 116306, August 2008.
2. Chenevert, M.E., “Shale Control With Balanced Activity Oil-Continuous Muds, “*J. Pet. Tech.* Oct 1970
3. Al-Bazali, T.M., “Experimental Study of the Membrane Behavior of Shale During Interaction with Water-base and Oil-Based Muds”, Dissertation presented to the Faculty of the Graduate School of The University of Texas at Austin, Austin, Texas, May, 2005
4. Abrams A., “Mud design to minimize rock impairment due to particle invasion”, *JPT* , May 1977
5. Dewan J., Chenevert M. E., “A model for filtration of water based mud during drilling: Determination of mudcake parameters”, *Petrophysics*, Vol 42, No. 3, May-June 2001